Zoosyst. Evol. 100 (3) 2024, 821–840 | DOI 10.3897/zse.100.121512

PENSOFT

MUSEUM FÜR NATURKUNDE BERLIN

Integrative taxonomy of *Dicellophilus* Cook, 1896 (Chilopoda, Geophilomorpha, Mecistocephalidae) in Japan, with a description of a new species

Sho Tsukamoto[1], Katsuyuki Eguchi[1,2]

1 *Systematic Zoology Laboratory, Graduate School of Science, Tokyo Metropolitan University, Minami-osawa 1-1 Hachioji-shi, Tokyo 192-0397, Japan*

2 *Department of International Health and Medical Anthropology, Institute of Tropical Medicine, Nagasaki University, 1-12-4 Sakamoto, Nagasaki 852-8523, Japan*

https://zoobank.org/B0AF778B-E394-4C17-910D-FA2BDFB14A4F

Corresponding author: Sho Tsukamoto (esutukamoto153@gmail.com)

Academic editor: Pavel Stoev ♦ **Received** 23 February 2024 ♦ **Accepted** 7 May 2024 ♦ **Published** 19 June 2024

Abstract

The genus *Dicellophilus* Cook, 1896, is a peculiar genus from the point of view of distribution. *Dicellophilus* is distributed in three limited areas that are well separated from one another: central Europe (*D. carniolensis*), Honshu (*D. pulcher*), and the southwestern part of the USA (*D. anomalus* and *D. limatus*). In the present study, in a field survey conducted throughout Japan, specimens belonging to the genus *Dicellophilus* were collected from Tohoku to the Kansai region, Honshu. Morphological analysis, molecular phylogenetic analysis, and genetic distance among *Dicellophilus* in Japan and *D. carniolensis* revealed that specimens from Sendai-shi, Miyagi Pref., could be assigned to an undescribed species. This previously unrecognized species is herein described as *D. praetermissus* **sp. nov.** The new species can be distinguished from *D. carniolensis* and *D. limatus* by the number of pairs of legs (43 pairs in *D. carniolensis* and 45 in *D. limatus*, but 41 in *D. praetermissus* **sp. nov.**), from *D. anomalus* by the lack of a pair of setae on the posteromedian part of the clypeus and variable crenulation on the internal margin of the forcipular tarsungulum, and from *D. pulcher* based on the following combination of characteristics: both ends of the transverse suture not evidently convex forward; long rather than wide trochanteroprefemur; wide rather than long metasternite.

Key Words

Cryptic species, DNA barcoding, geophilomorph centipede, molecular, phylogeny

Introduction

The geophilomorph family Mecistocephalidae Bollman, 1893, is mainly distributed from temperate to tropical regions in both hemispheres, and species diversity is remarkably high in Japan (Uliana et al. 2007; Bonato 2011). To date, approximately 180 species are known worldwide, and 31 species have been recorded from Japan (Uliana et al. 2007; Tsukamoto et al. 2019, 2022). Therefore, approximately 20% of all known mecistocephalid species are distributed in Japan. Moreover, Japan is the richest with regard to the number of genera (nine out of 11 genera; Uliana et al. 2007; Tsukamoto et al. 2022).

Mecistocephalidae are morphologically characterized by a cephalic capsule and a forcipular segment that are evidently sclerotized and darker than the remaining trunk segments (Bonato et al. 2003, 2014; Uliana et al. 2007; Bonato 2011). In addition, the following three features characterize Mecistocephalidae: a mandible with a series of pectinate lamellae only; trunk sternites with an internal apodeme; and a mid-longitudinal sulcus (Bonato et al. 2003). Notably, the segment number of most species of Mecistocephalidae has no intraspecific variation, except for some species of the genus *Mecistocephalus* Newport, 1843, with a very high number of leg-bearing segments (Bonato et al. 2003, 2014; Uliana et al. 2007; Bonato 2011).

Among Mecistocephalidae, the genus *Dicellophilus* Cook, 1896, is a distinct genus from a morphological viewpoint, with the following diagnostic characteristics: a macropore near the center of the coxopleuron and a concave margin of the lateral side pieces of the labrum (Uliana et al. 2007; Bonato et al. 2010a). See table 2 of Bonato et al. (2010a) and table 1 of Dyachkov and Bonato (2022) for diagnostic characteristics of the genus *Dicellophilus*. To date, four valid species have been known in the genus *Dicellophilus*, namely, *D. carniolensis* (C.L. Koch, 1847), *D. pulcher* (Kishida, 1928), *D. anomalus* (Chamberlin, 1904), and *D. limatus* (Wood, 1862).

The distribution of *Dicellophilus* is limited to three areas that are well separated from one another: central Europe (*D. carniolensis*), Honshu of Japan (*D. pulcher*), and the southwestern part of the USA (*D. anomalus* and *D. limatus*) (Bonato et al. 2003, 2010a). All three distribution areas are located within a narrow latitudinal band, at approximately 35–45°N, and all species inhabit humid litter and soil in forests (Bonato et al. 2010a).

Bonato et al. (2010a) performed phylogenetic analyses of the genus *Dicellophilus* with a morphological dataset consisting of 30 characteristics and indicated that the two American species, viz., *D. anomalus* and *D. limatus*, were sister species, and *D. pulcher* formed a clade with the two American species. As far as extant species are concerned, *D. carniolensis* is thus the first diverged species in the genus *Dicellophilus*.

For a decade, the combination of morphological observation, molecular phylogenetic analyses, and DNA barcoding ("integrative taxonomy") has helped detect undescribed species and reveal the genetic structure of the taxa concerned (Dayrat 2005; Padial et al. 2010). For example, some studies using integrative approaches to scolopendromorphs and geophilomorphs have revealed the existence of many cryptic species under one validly named species or distinct morphospecies (Joshi and Karanth 2012; Siriwut et al. 2015, 2016; Tsukamoto et al. 2021b; Peretti et al. 2022; Bonato et al. 2023). Tsukamoto et al. (2022) also detected the existence of two species of the mecistocephalid genus *Nannarrup* Foddai, Bonato, Pereira & Minelli, 2003 by using an integrative approach.

Inspired by these previous studies, the present study aims to reveal the genetic diversity and confirm whether the morphospecies *D. pulcher* involves unnoticed and undescribed cryptic species by using an integrative taxonomic approach.

Materials and methods

Taxon sampling

Although our ongoing sampling efforts to taxonomically reveal the East Asian mecistocephalid faunas cover the whole of Japan and surrounding areas, the present study focused on Honshu (the largest island of mainland Japan), from which *D. pulcher* was described.

A total of 38 specimens morphologically identified as *Dicellophilus pulcher*, hitherto the only known Japanese species of the genus, were collected from Honshu from 2018 to 2021. The detailed collection sites of the examined specimens are shown in Fig. 1, Table 1, and the "Taxonomic account" section. The altitude data provided by AW3D of JAXA (https://www.eorc.jaxa.jp/ALOS/jp/index_j.htm) and the coastal line provided by the digital nation land information (https://nlftp.mlit.go.jp/index.html) were used to generate Fig. 1.

Each specimen was labeled with its unique specimen identification number in the form "TSYYYYMMDD-XX," where TS is an abbreviation of the first author's name, Tsukamoto Sho; YYYYMMDD designates the date on which the specimen was collected; and XX is the identification number assigned to each specimen collected on a particular date (e.g., TS20171010-01).

All of the type specimens of *Dicellophilus* designated in this paper were deposited at the Collection of Myriapoda, Department of Zoology, National Museum of Nature and Science, Tokyo (NSMT), and the Museum of Nature and Human Activities, Hyogo (MNHAH). The deposition site of each type specimen is shown in the "Taxonomic account" section. All non-type voucher specimens of *Dicellophilus pulcher* are managed by the first author.

Morphological examination

For dissected specimens, the cephalic capsule, maxillae, mandibles, forcipular segment, and leg-bearing segments were made transparent using lactic acid to examine the anatomy and produce images. Multi-focused images of these body parts were produced using Affinity Photo 1.10.4 (https://affinity.serif.com/ja-jp/photo/) from a series of source images taken using a Canon EOS Kiss X9 digital camera attached to a Nikon AZ100 microscope and improved using Adobe Photoshop Elements 10 and Affinity Designer 1.10.5 (https://affinity.serif.com/ja-jp/designer/). Then, the body parts were measured directly using an ocular micrometer attached to the microscope.

The morphological terminology used in this study is in accordance with Bonato et al. (2010b). Specimens with fully developed paired gonopods, that is, evidently biarticulated in males and touching one another in females, were determined to be adults, and those with incompletely developed paired gonopods were determined to be subadults. Specimens without gonopods were determined to be juveniles based on Uliana et al. (2007). In the present study, 23 adult specimens out of 38 collected were examined morphologically.

DNA sequencing

Genomic DNA was extracted from one or two legs of each specimen in accordance with the Chelex-TE-ProK protocol described by Satria et al. (2015), with incubation for 4–24 h.

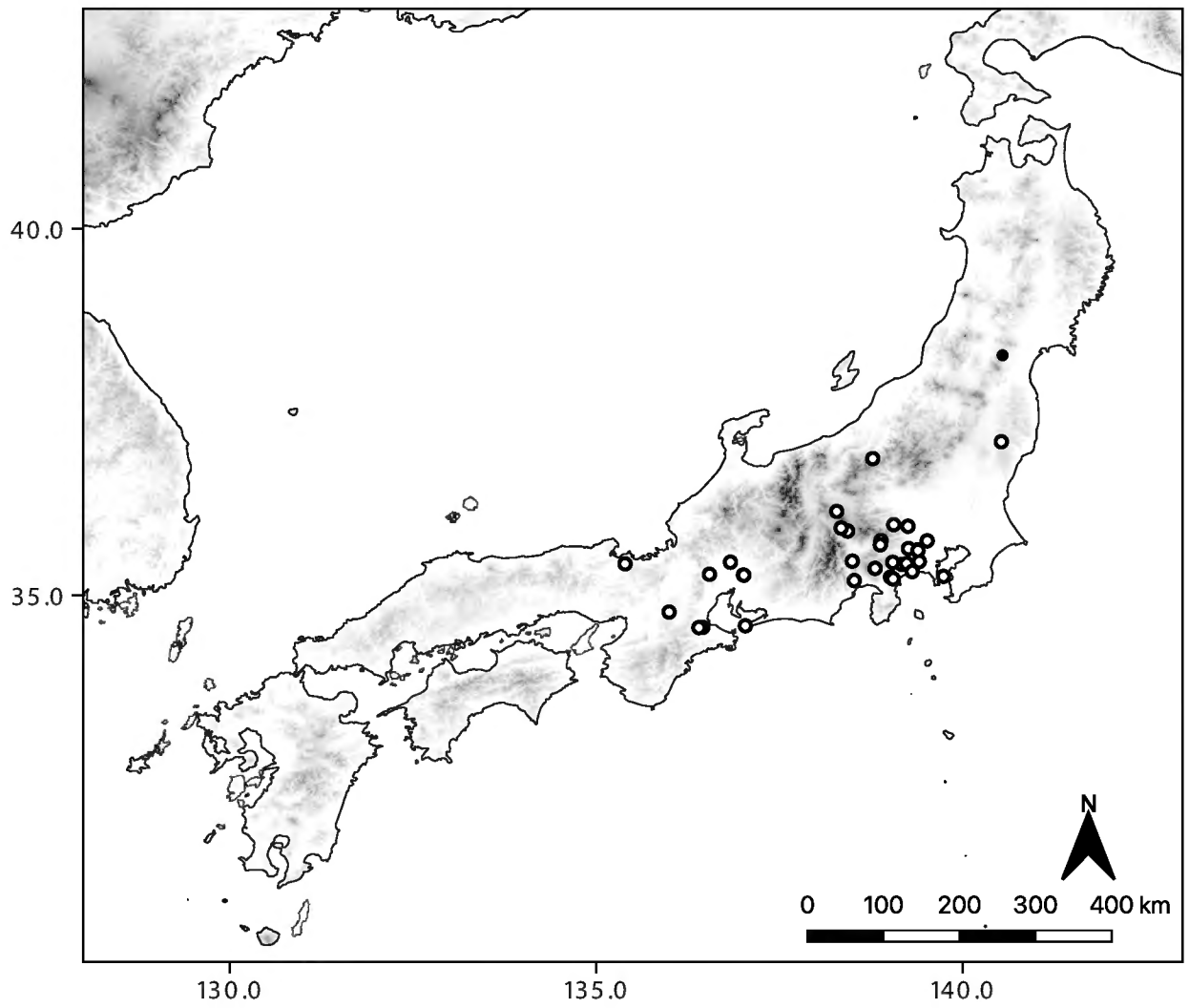

Figure 1. Map of the collection sites of specimens examined in the present study. White circle, *Dicellophilus pulcher*; black circle, *D. praetermissus* sp. nov.

PCR amplification was performed in a MiniAmp Thermal Cycler (Thermo Fisher Scientific, Waltham, Massachusetts, USA) in a 10.5-μL reaction volume containing 5 μL of 2× PCR buffer for KOD FX Neo, 2 μL of 2 mM dNTPs, 0.3 μL of 10 pmol/μL forward and reverse primers, 0.2 μL of 1.0 U/μL DNA polymerase KOD FX Neo (TOYOBO KFX-201X5), and 1.0 μL of DNA template. The sequences of primers for mitochondrial cytochrome *c* oxidase subunit I (*COI*), *16S rRNA* (*16S*), and nuclear *28S rRNA* (*28S*) genes are shown in Table 2. Each PCR product was screened by electrophoresis on a 2.0% agarose gel in 1× TAE.

The amplification conditions for mitochondrial *COI* were as follows: 98 °C for 2 min; 5 cycles of 98 °C for 10 s; 45 °C for 30 s; and 68 °C for 45 s; 40 cycles of 98 °C for 10 s; 48.5 °C for 30 s (annealing step); 68 °C for 45 s; and 68 °C for 7 min. If the target fragment of *COI* was not appropriately amplified, then the annealing temperature was changed from 48.5 °C to 50 °C. PCR was performed again by omitting the first five cycles of annealing and the extension step.

The amplification conditions for mitochondrial *16S* were as follows: 98 °C for 2 min; 35 cycles of 98 °C for 10 s; 45 °C for 30 s (annealing step); 68 °C for 45 s; and 68 °C for 7 min. If the target fragment of *16S* was not appropriately amplified, then the annealing temperature was changed from 45 °C to 48 °C. The number of annealing cycles was changed from 35 to 45.

The amplification conditions for nuclear *28S* were as follows: 98 °C for 2 min; 5 cycles of 98 °C for 10 s; 42 °C for 30 s; and 68 °C for 1 min; 30 cycles of 98 °C for 10 s; 50 °C for 30 s (annealing step); 68 °C for 1 min; and 68 °C for 7 min. If the target fragment of *28S* was not appropriately amplified, then the annealing temperature was changed from 50 °C to 48 °C. The number of annealing cycles was changed from 30 to 40–45 cycles. In addition, PCR was performed again by omitting the first five cycles of annealing and the extension step.

The amplified products were incubated at 37 °C for 4 min and at 80 °C for 1 min using ExoSAP-IT™ Express (Thermo Fisher Scientific) to remove any excess primers and nucleotides. All nucleotide sequences were determined by direct sequencing using the ABI PRISM BigDye™ Terminator Cycle Sequencing Kit ver. 3.1 (Thermo Fisher Scientific) or BrilliantDye™ Terminator Cycle Sequencing Kit v. 3.1 (Nimagen, B.V., Nijmegen, Netherlands) equipped with an ABI 3130xl automated sequencer (Thermo Fisher Scientific). The sequences were assembled using ChromasPro 1.7.6 (Technelysium Pty Ltd., Australia) and deposited onto the DDBJ, EMBL, and GenBank databases under the accession numbers LC815125– LC815233 (Table 1).

Molecular phylogenetic analyses

The sequences obtained using the abovementioned methods were used for phylogenetic analyses, together with the *COI*, *16S*, and *28S* sequences of *Dicellophilus carniolensis* (C.L. Koch, 1847) and *Nannarrup innuptus* Tsukamoto in Tsukamoto et al. (2022) obtained from GenBank as outgroups (Table 1). The datasets for *COI* (658 bp positions), *16S* (514 bp positions), and *28S* (971 bp positions) were concatenated to form the *COI* + *16S* + *28S* dataset for phylogenetic analyses.

Table 1. The list of specimens that were used in the phylogenetic analyses. Geographic coordinates enclosed by parentheses are secondary due to the lack of information in the labels.

Specimen ID	Geographic coordinate of collection sites	Sequence data (Accession no.)			Remarks
		COI	*16S*	*28S*	
***Dicellophilus pulcher* (Kishida, 1928)**					
TS20220518-01	35°16.45'N, 137°00.59'E (Aichi Pref.)	LC815129	LC815167	LC815205	Tomoki Sumino leg.
TS20210809-01	34°33.71'N, 136°27.33'E (Mie Pref.)	LC815130	LC815168	LC815206	Tomoki Sumino & Fukube Sumino leg.
TS20210809-02	34°33.71'N, 136°27.33'E (Mie Pref.)	LC815131	LC815169	LC815207	Tomoki Sumino & Fukube Sumino leg.
TS20220813-01	34°33.42'N, 136°24.13'E (Mie Pref.)	LC815132	LC815170	LC815208	Tomoki Sumino leg.
TS20230517-01	35°16.38'N, 137°00.96'E (Aichi Pref.)	LC815133	LC815171	LC815209	Tomoki Sumino leg.
TS20190413-01	35°25.15'N, 139°10.39'E (Kanagawa Pref.)	LC815134	LC815172	LC815210	Sho Tsukamoto leg.
TS20181214-01	35°37.02'N, 139°22.74'E (Tokyo Pref.)	LC815135	LC815173	–	Joe Kutsukake leg.
TS20180714-01	35°27.46'N, 139°24.51'E (Kanagawa Pref.)	LC815136	LC815174	–	Joe Kutsukake leg.
TS20191006-02	35°38.15'N, 139°15.71'E (Tokyo Pref.)	LC815137	LC815175	–	Sho Tsukamoto leg.
TS20200924-01	35°52.42'N, 138°25.96'E (Yamanashi Pref.)	LC815138	–	–	Joe Kutsukake leg.
TS20200927-01	35°54.95'N, 138°20.55'E (Yamanashi Pref.)	LC815139	LC815176	–	Koshi Kawamoto leg.
TS20201122-01	(35°25.62'N, 135°23.69'E) (Kyoto Pref.)	LC815140	LC815177	LC815211	Tatsumi Suguro leg.
TS20210322-01	35°15.40'N, 139°44.43'E (Kanagawa Pref.)	LC815141	LC815178	–	Ryo Miyata leg.
TS20210401-03	35°44.46'N, 139°31.01'E (Tokyo Pref.)	LC815142	LC815179	LC815212	Mayu Susukida leg.
TS20210411-08	35°26.84'N, 139°02.82'E (Kanagawa Pref.)	LC815143	LC815180	LC815213	Namiki Kikuchi leg.
TS20210424-07	35°25.88'N, 139°14.15'E (Kanagawa Pref.)	LC815144	LC815181	LC815214	Katsuyuki Eguchi leg.
TS20210504-01	35°21.91'N, 138°48.44'E (Shizuoka Pref.)	LC815145	LC815182	LC815215	A topotype of *D. pulcher*; Sho Tsukamoto leg.
TS20210418-01	34°34.94'N, 137°02.13'E (Aichi Pref.)	LC815146	LC815183	LC815216	Katsuyuki Eguchi leg.
TS20210522-01	35°44.78'N, 138°53.15'E (Yamanashi Pref.)	LC815147	LC815184	LC815217	Takahiro Yoshida leg.
TS20210530-02	35°41.19'N, 138°52.64'E (Yamanashi Pref.)	LC815148	LC815185	LC815218	Namiki Kikuchi leg.
TS20210722-01	35°57.71'N, 139°03.60'E (Saitama Pref.)	LC815149	LC815186	LC815219	Mayu Susukida leg.
TS20211004-01	(36°08.54'N, 138°16.92'E) (Nagano Pref.)	LC815150	LC815187	LC815220	Masaru Nonaka leg.
TS20211030-04	36°51.75'N, 138°46.43'E (Niigata Pref.)	LC815151	LC815188	LC815221	Katsuyuki Eguchi leg.
TS20211018-02	35°26.99'N, 136°49.95'E (Gifu Pref.)	LC815152	LC815189	LC815222	Katsuyuki Eguchi leg.
TS20210919-01	34°46.18'N, 135°59.73'E (Kyoto Pref.)	LC815153	LC815190	LC815223	Katsuyuki Eguchi leg.
TS20210711-15	35°17.08'N, 136°32.74'E (Gifu Pref.)	LC815154	LC815191	LC815224	Katsuyuki Eguchi leg.
TS20210819-01	35°36.51'N, 139°23.48'E (Tokyo Pref.)	LC815155	LC815192	LC815225	Katsuyuki Eguchi leg.
TS20210523-01	35°27.82'N, 138°29.66'E (Yamanashi Pref.)	LC815156	LC815193	LC815226	Katsuyuki Eguchi leg.
TS20210531-01	37°05.59'N, 140°31.72'E (Fukushima Pref.)	LC815157	LC815194	LC815227	Katsuyuki Eguchi leg.
TS20210523-03	35°11.94'N, 138°31.29'E (Shizuoka Pref.)	-	LC815195	LC815228	Katsuyuki Eguchi leg.
TS20210718-01	35°56.36'N, 139°15.30'E (Saitama Pref.)	LC815158	LC815196	LC815229	Katsuyuki Eguchi leg.
TS20210508-02	35°19.27'N, 139°18.72'E (Kanagawa Pref.)	LC815159	LC815197	LC815230	Katsuyuki Eguchi leg.
TS20210531-02	37°05.59'N, 140°31.72'E (Fukushima Pref.)	LC815160	LC815198	LC815231	Katsuyuki Eguchi leg.
TS20210728-01	35°14.75'N, 139°01.02'E (Kanagawa Pref.)	LC815161	LC815199	LC815232	Sho Tsukamoto leg.
TS20210728-02	35°13.32'N, 139°03.13'E (Kanagawa Pref.)	LC815162	LC815200	LC815233	Sho Tsukamoto leg.
***Dicellophilus praetermissus* sp. nov.**					
TS20201007-02	38°16.33'N, 140°32.69'E (Miyagi Pref.)	LC815125	LC815163	LC815201	Sho Tsukamoto leg.
TS20201007-03	38°16.33'N, 140°32.69'E (Miyagi Pref.)	LC815126	LC815164	LC815202	Sho Tsukamoto leg.
TS20201007-04	38°16.33'N, 140°32.69'E (Miyagi Pref.)	LC815127	LC815165	LC815203	Sho Tsukamoto leg.
TS20201007-05	38°16.33'N, 140°32.69'E (Miyagi Pref.)	LC815128	LC815166	LC815204	Sho Tsukamoto leg.
***Dicellophilus carniolensis* (Koch, 1847) (outgroup)**					
DNA102580/LBv792	No data	KF569305	HM453225	HM453285	Referred from Murienne et al. (2010), Bonato et al. (2014)
***Nannarrup innuptus* Tsukamoto in Tsukamoto et al. 2022 (outgroup)**					
TS20210503-09	34°51.39'N, 138°55.40'E (Shizuoka Pref.)	LC715530	LC715605	LC715680	Referred from Tsukamoto et al. (2022)

All sequences were aligned using MAFFT v. 7.475 (Katoh and Standley 2013). For *COI*, alignment was performed using the default setting. For *16S* and *28S*, secondary structure alignment was performed using the X-INS-i option.

Maximum-likelihood (ML) trees were created on the basis of the sequence dataset for each gene and concatenated using IQ-tree 1.6.12 (Nguyen et al. 2015). As an optimal substitution model in accordance with BIC, TNe + I + G4 was selected for the first codon position

Table 2. The list of primers used in the present study.

Genes	Primer name	Sequence (5' - 3')	Source
COI	LCO-CH	TTT CAA CAA AYC AYA AAG ACA TYG G	Tsukamoto et al. (2021a)
	HCO-CH	TAA ACT TCT GGR TGR CCR AAR AAT CA	
16S rRNA	16Sa	CGC CTG TTT ATC AAA AAC AT	Xiong and Kocher (1991)
	16Sbi	CTC CGG TTT GAA CTC AGA TCA	
28S rRNA	28S D1F	GGG ACT ACC CCC TGA ATT TAA GCA T	Boyer and Giribet (2007)
	28S rD4b	CCT TGG TCC GTG TTT CAA GAC	Edgecombe and Giribet (2006)

of *COI* in the concatenated dataset; TNe + G4 for the *COI* dataset; HKY + F was selected for the second codon position of *COI* in both datasets; TN + F + G4 was selected for the third codon position of *COI* in both datasets; HKY + F + I + G4 was selected for *16S* of both datasets; and TIM3e + G4 was selected for *28S* of both datasets. Ultrafast bootstrap analysis (UFBoot; Hoang et al. 2018) and the SH-like approximate likelihood ratio test (SH-aLRT; Guindon et al. 2010) were performed with 1,000 replicates.

Bayesian inference trees were created using ExaBayes 1.4.1 (Aberer et al. 2014) under the default substitution model "GTR + G." The Markov chain Monte Carlo method was used with random starting trees and performed once for each of the four chains (three hot and one cold) for 10,000,000 generations for each dataset except *COI*, but for 20,000,000 generations for the *COI* dataset. Trees were sampled every 500 generations, tuning parameters every 100 generations, and the first 25% of the trees were discarded as burn-in. Other parameters were set in accordance with the default settings. The effective sampling size of each parameter was confirmed to be 200 using Tracer 1.7.1 (Rambaut et al. 2018).

Calculation of the genetic distances

The aligned *COI* dataset used for phylogenetic analyses were also used to calculate genetic distances. Kimura two-parameter (K2P) distances were calculated using MEGA X (Kumar et al. 2018) with the setting "pairwise deletion."

Delimitation of "provisional" operational taxonomic units

The program "assemble species by automatic partitioning (ASAP)" was used to delimit "provisional" operational taxonomic units (POTUs). ASAP is a species delimitation program based on a hierarchical clustering algorithm that only uses pairwise genetic distances (Puillandre et al. 2021; available at https://bioinfo.mnhn.fr/abi/public/asap/). ASAP was performed for the *COI* sequence dataset of *Dicellophilus* (excluding the outgroup) under the "pairwise K2P distance" method.

Delimitation of putative species and provisional naming of each putative species

The present study preliminarily relied on the morphological information provided by Bonato et al. (2010a) as the basis for the monophyly of the genus *Dicellophilus*. Then, putative species were proposed. Except for the assumption of monophyly of the abovementioned genus, the following steps generally followed the workflow "DI-system" proposed by the first author in Tsukamoto (2023) for discriminating and labeling putative species: (I) sorting specimens, which are morphologically conferrable to *Dicellophilus*, into morphospecies; (II) confirming the monophyly of the morphospecies with the phylogenetic tree inferred by the sequence dataset of three gene markers, mitochondrial *COI* and *16S*, and nuclear *28S*; (III) calculating the genetic distance of *COI* between congeneric morphospecies, which are confirmed to be monophyletic, to define the intermorphospecific threshold; (IV) delimiting POTUs using ASAP (see above) and confirming the most conferrable hypotheses of species-level independence by considering the phylogenetic tree and the intermorphospecific threshold defined in step III. By steps III and IV, species hypotheses can be established from two viewpoints, viz., phylogeny and clustering based on DNA data. In step IV, putative species were recognized by considering three species delimitation principles: (1) each clade is regarded as an independent putative species if it diverges from all others with a minimum K2P distance higher than the intermorphospecific threshold; (2) a single putative species that satisfies (1) can contain inner lineage(s) diverging extremely from the others unless the maximum distance from the sister inner lineage exceeds the intermorphospecific threshold; (3) a single putative species that satisfies (2) cannot contain inner lineage(s) diverging extremely from the sister inner lineage with the minimum K2P distance exceeding the intermorphospecific threshold, and such a lineage must be further considered as a distinct species if it exists.

As mentioned above, the present study presupposes the monophyly of *Dicellophilus*, supported by the morphological evidence (Bonato et al. 2010a). This is because the possibility of a difference in evolutionary rate among genera is important for defining the intermorphospecific threshold in the "DI-system". "DI-system" is planned to be proposed formally in future studies.

Each putative species recognized by following the abovementioned steps was also labeled in accordance with the study of Tsukamoto (2023), with a unique, permanent, and citable identifier "DI," such as "0000-0003-3020-8454_XXXX," in which "0000-0003-3020-8454" shows the author's ORCID and "XXXX" shows a unique identification number given to each species in the author's life-long research. ORCIDs involved in the species identification codes were omitted except for section titles, figure legends, and tables to avoid redundancy.

Depending on the availability of the morphological information necessary to formally describe and name species in the conventional manner of Linnaean Taxonomy (The International Commission on Zoological Nomenclature 1999), the putative species labeled with the DI can be described and named (step V). In the present study, species discrimination (steps I–IV) and formal description and naming of the species (step V) were separated as two methodologically distinct phases.

Results

Molecular phylogenetic analyses

COI was successfully sequenced for 38 specimens, *16S* for 38 specimens, and *28S* for 33 specimens (Table 1). The ML tree based on the concatenated dataset (Fig. 2) and BI tree based on the same dataset (only show the posterior probability in Fig. 2) involving 39 specimens shows that the clade consisting of TS20201007-02, TS20201007-03, TS20201007-04, and TS20201007-05 from Miyagi Pref. (UFBoot = 100%, SH-aLRT = 100%, posterior probability (PP) = 1.00; hereafter referred to as "Clade A") is deeply separated from the clade consisting of all other *Dicellophilus* specimens collected in Japan and the European species *D. carniolensis* (UFBoot = 95.4%, SH-aLRT = 98%, PP = 1.00). The monophyly of the clade, which consists of the remaining *Dicellophilus* specimens from Japan, was strongly supported (UFBoot = 100%, SH-aLRT = 100%,

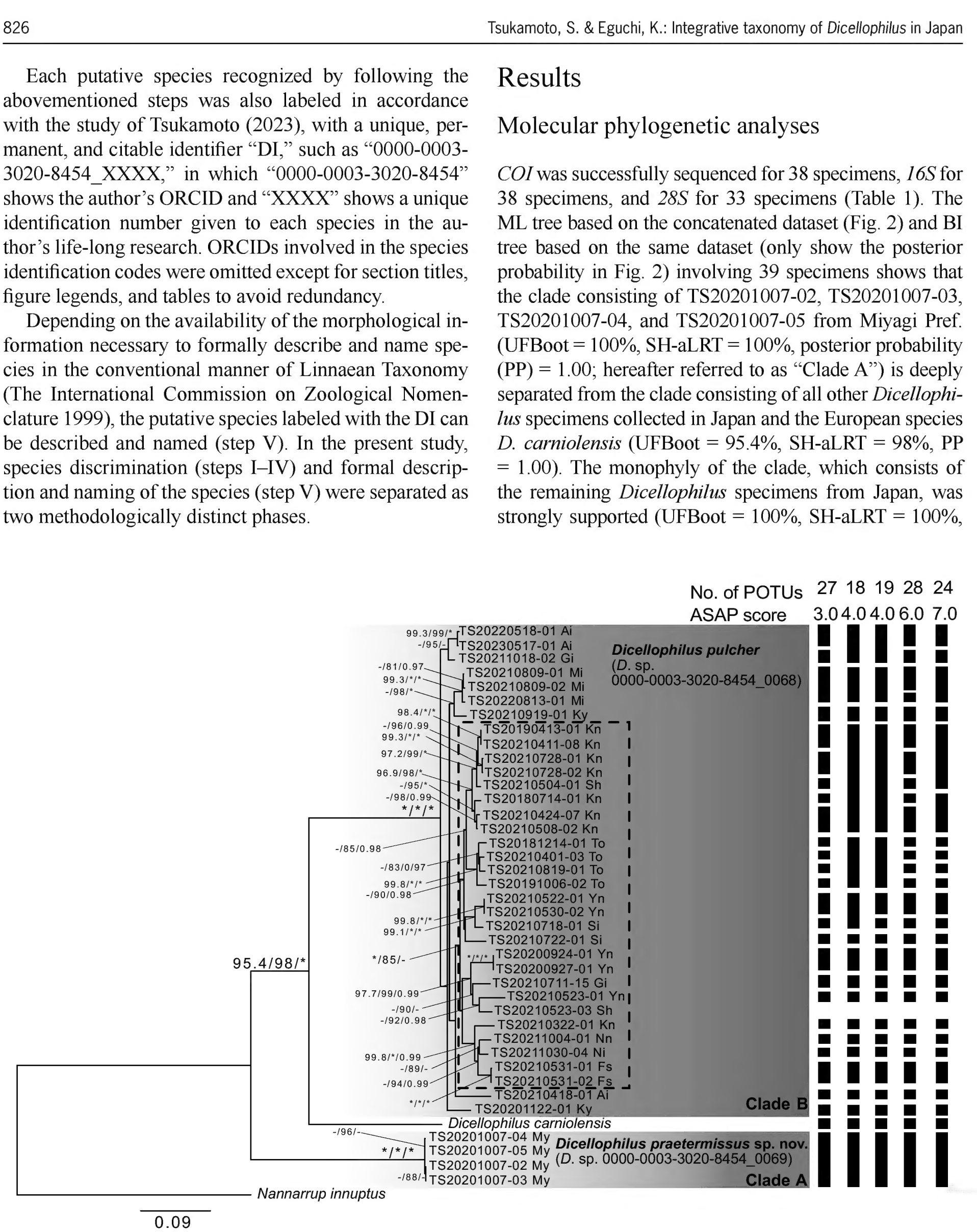

Figure 2. Maximum-likelihood tree of *Dicellophilus* based on the concatenated dataset of *COI*, *16S*, and *28S*, with the results of species delimitation by ASAP. Note that specimens whose *COI* sequence was not determined were included in the conferred species if they belonged to the same concerning clade to easily understand the result of species delimitation. Nodal values are obtained from the ultrafast bootstrap (UFBoot), SH-like approximate likelihood ratio test (SH-aLRT), and posterior probability (PP). The asterisk (*) indicates 100% in UFBoot, SH-aLRT, and 1.0 in PP. Hyphen (-) indicates lower than 95% in UFBoot, 80% in SH-aLRT, or 0.95 in PP. Nodal values are not shown when UFBoot, SH-aLRT, and PP values are <95%, <80%, and <0.95, respectively. The unit of evolutionary distance is the number of base substitutions per site. A broken square shows that the clade consisted of specimens from eastern Honshu. Abbreviations: Ai = Aichi Pref.; Fs = Fukushima Pref.; Gi = Gifu Pref.; Kn = Kanagawa Pref.; Ky = Kyoto Pref.; Mi = Mie Pref.; My = Miyagi Pref.; Ni = Niigata Pref.; Nn = Nagano Pref.; Sh = Shizuoka Pref.; Si = Saitama Pref.; To = Tokyo Pref.; Yn = Yamanashi Pref.

PP = 1.00; hereafter "Clade B"), and notably, specimens from Eastern Honshu (Fukushima Pref. to Shizuika Pref., and one specimen from Gifu Pref.) formed a clade with a high support value (UFBoot = 100%, SH-aLRT = 85%, PP = 0.91; enclosed by a broken square in Fig. 2). On the contrary, the monophyly of specimens from western Honshu (Gifu Pref. to Kyoto Pref.) was not supported.

The ML tree based on the *COI* dataset (Fig. 3) and the BI tree based on the same dataset (only PP shown in Fig. 3) involving 38 specimens also show Clade A (UFBoot = 99.6%, SH-aLRT = 100%, PP = 1.00). Although Clade A forms a further clade with *D. carniolensis* (UFBoot = 99.6%, SH-aLRT = 100%, PP = 1.00), Clade A is deeply separated from clade B (UFBoot = 90.8%, SH-aLRT = 95%, PP = 1.00). In addition, the monophyly of specimens from western Honshu in Clade B (Gifu Pref. to Kyoto Pref.) was moderately supported (UFBoot = 88.2%, SH-aLRT = 88%, PP = 0.98; enclosed by a broken square in Fig. 3), but that of eastern Honshu was not supported.

The ML tree based on the *16S* dataset (Fig. 4) and the BI tree based on the same dataset (only PP shown in Fig. 4) involving 38 specimens also show Clade A (UFBoot = 100%, SH-aLRT = 100%, PP = 1.00). Clade A is deeply separated from all other *Dicellophilus* specimens, but Clade B is not well supported (UFBoot = 78.2%, SH-aLRT = 63%, PP = 0.91). In addition, the phylogenetic relationship among Clade B and other *Dicellophilus* specimens was not clear due to low support values.

The ML tree based on the *28S* dataset (Fig. 5) and the BI tree based on the same dataset (only PP shown in Fig. 5) involving 33 specimens also show Clade A (UFBoot = 99.7%, SH-aLRT = 100%, PP = 1.00). Clade A is deeply separated from all other *Dicellophilus* specimens, and Clade B conforms to a further clade with *D. carniolensis*, like the topology of the concatenated dataset (UFBoot = 93.6%, SH-aLRT = 97%, PP = 0.99). However, the phylogenetic relationship among Clade B and other *Dicellophilus* specimens was not clear due to low support values.

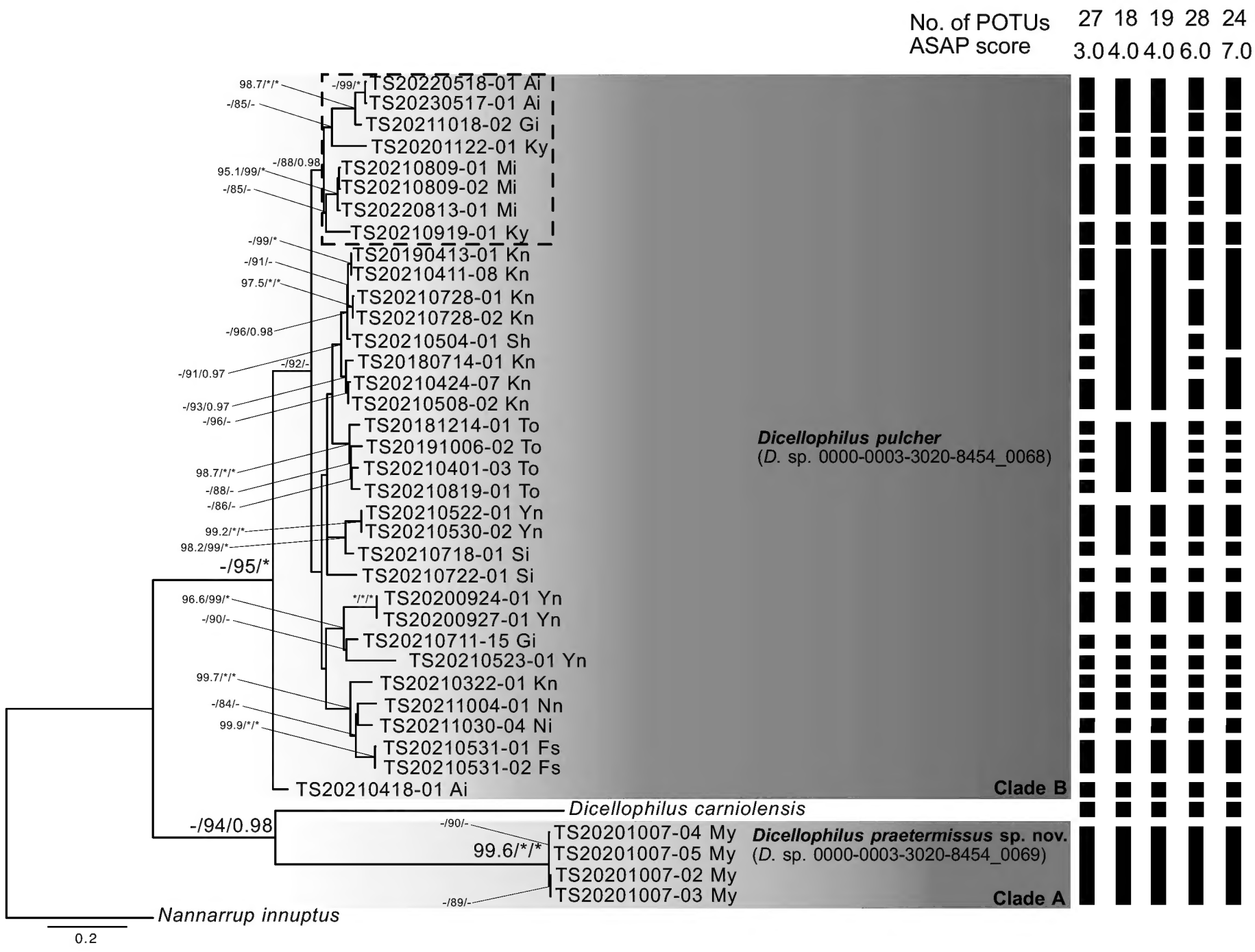

Figure 3. Maximum-likelihood tree of *Dicellophilus* based on the dataset of *COI*, with the results of species delimitation by ASAP. Nodal values are obtained from the ultrafast bootstrap (UFBoot), SH-like approximate likelihood ratio test (SH-aLRT), and posterior probability (PP). The asterisk (*) indicates 100% in UFBoot, SH-aLRT, and 1.0 in PP. Hyphen (-) indicates lower than 95% in UFBoot, 80% in SH-aLRT, or 0.95 in PP. Nodal values are not shown when UFBoot, SH-aLRT, and PP values are <95%, <80%, and <0.95, respectively. The unit of evolutionary distance is the number of base substitutions per site. A broken square shows that the clade consisted of specimens from eastern Honshu. Abbreviations: Ai = Aichi Pref.; Fs = Fukushima Pref.; Gi = Gifu Pref.; Kn = Kanagawa Pref.; Ky = Kyoto Pref.; Mi = Mie Pref.; My = Miyagi Pref.; Ni = Niigata Pref.; Nn = Nagano Pref.; Sh = Shizuoka Pref.; Si = Saitama Pref.; To = Tokyo Pref.; Yn = Yamanashi Pref.

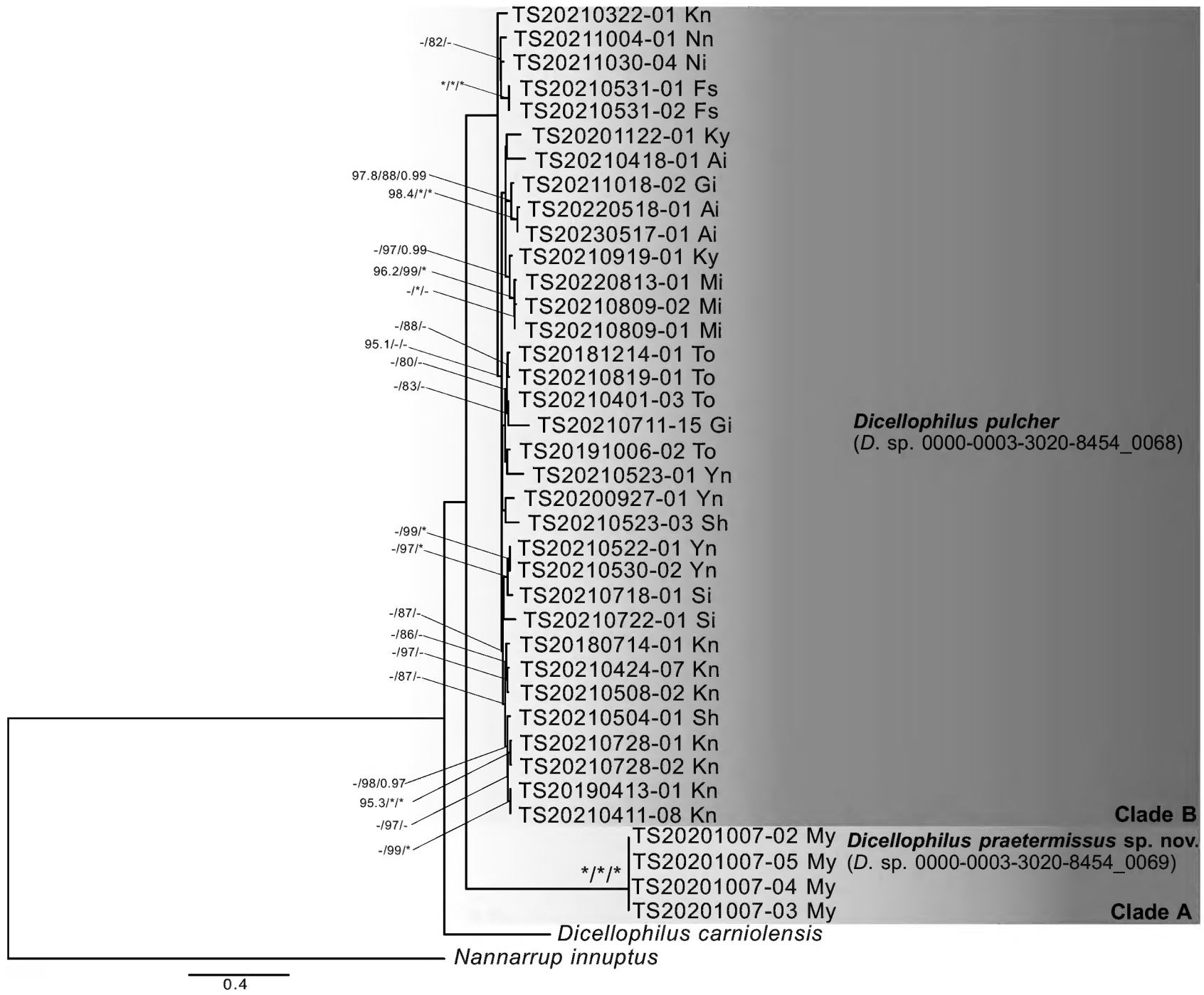

Figure 4. Maximum-likelihood tree of *Dicellophilus* based on the dataset of *16S*. Nodal values are obtained from the ultrafast bootstrap (UFBoot), SH-like approximate likelihood ratio test (SH-aLRT), and posterior probability (PP). The asterisk (*) indicates 100% in UFBoot, SH-aLRT, and 1.0 in PP. Hyphen (-) indicates lower than 95% in UFBoot, 80% in SH-aLRT, or 0.95 in PP. Nodal values are not shown when UFBoot, SH-aLRT, and PP values are <95%, <80%, and <0.95, respectively. The unit of evolutionary distance is the number of base substitutions per site. A broken square shows that the clade consisted of specimens from eastern Honshu. Abbreviations: Ai = Aichi Pref.; Fs = Fukushima Pref.; Gi = Gifu Pref.; Kn = Kanagawa Pref.; Ky = Kyoto Pref.; Mi = Mie Pref.; My = Miyagi Pref.; Ni = Niigata Pref.; Nn = Nagano Pref.; Sh = Shizuoka Pref.; Si = Saitama Pref.; To = Tokyo Pref.; Yn = Yamanashi Pref.

Although there is no consistency of phylogenetic relationship among Clades A, B, and *D. carniolensis* in four datasets, each topology shows that Clade A is a distinct lineage from other *Dicellophilus* specimens.

Intermorphospecific threshold and POTU delimitation of *Dicellophilus* specimens

The minimum K2P distance between congeneric morphospecies was 21% (*D. carniolensis* (accession no.: KF569305) vs. *D. pulcher* TS20230517-01 from Aichi Pref.). Thus, the intermorphospecific threshold induced by this dataset is 21%. However, the maximum K2P distance was 24% within *D. pulcher* (TS20191006-02 from Tokyo Pref. in Clade B vs. TS20201007-04 from Miyagi Pref. in Clade A).

The maximum K2P distance within Clade A was 0.6% (TS20201007-04 vs. TS20201007-02 and TS20201007-03), and that within Clade B was 15% (TS20210322-01 from Kanagawa Pref. vs. TS20210523-01 from Yamanashi Pref.).

The best five partitioning hypotheses inferred by the ASAP program are shown in Figs 2, 3, with the following ASAP scores: (1) 27 POTUs with a score of 3.0; (2) 18 POTUs with a score of 4.0; (3) 19 POTUs with a score of 4.0; (4) 28 POTUs with a score of 6.0; and (5) 24 POTUs with a score of 7.0.

Morphological examination of Japanese *Dicellophilus*

All 38 specimens of *D. pulcher* (a combination of Clades A and B) examined in steps I–IV have 41 pairs of legs and can be distinguished from *D. carniolensis* and *D. limatus* by the number of pairs of legs (43 pairs in *D. carniolensis* and 45 in *D. limatus*). Examined 23 adult specimens can also be distinguished from *D. anomalus*, which has 41 pairs of legs, by the lack of a pair of setae on the posteromedian part of the clypeus and variable crenulation on the internal margin of the forcipular tarsungulum (Bonato et al. 2010a).

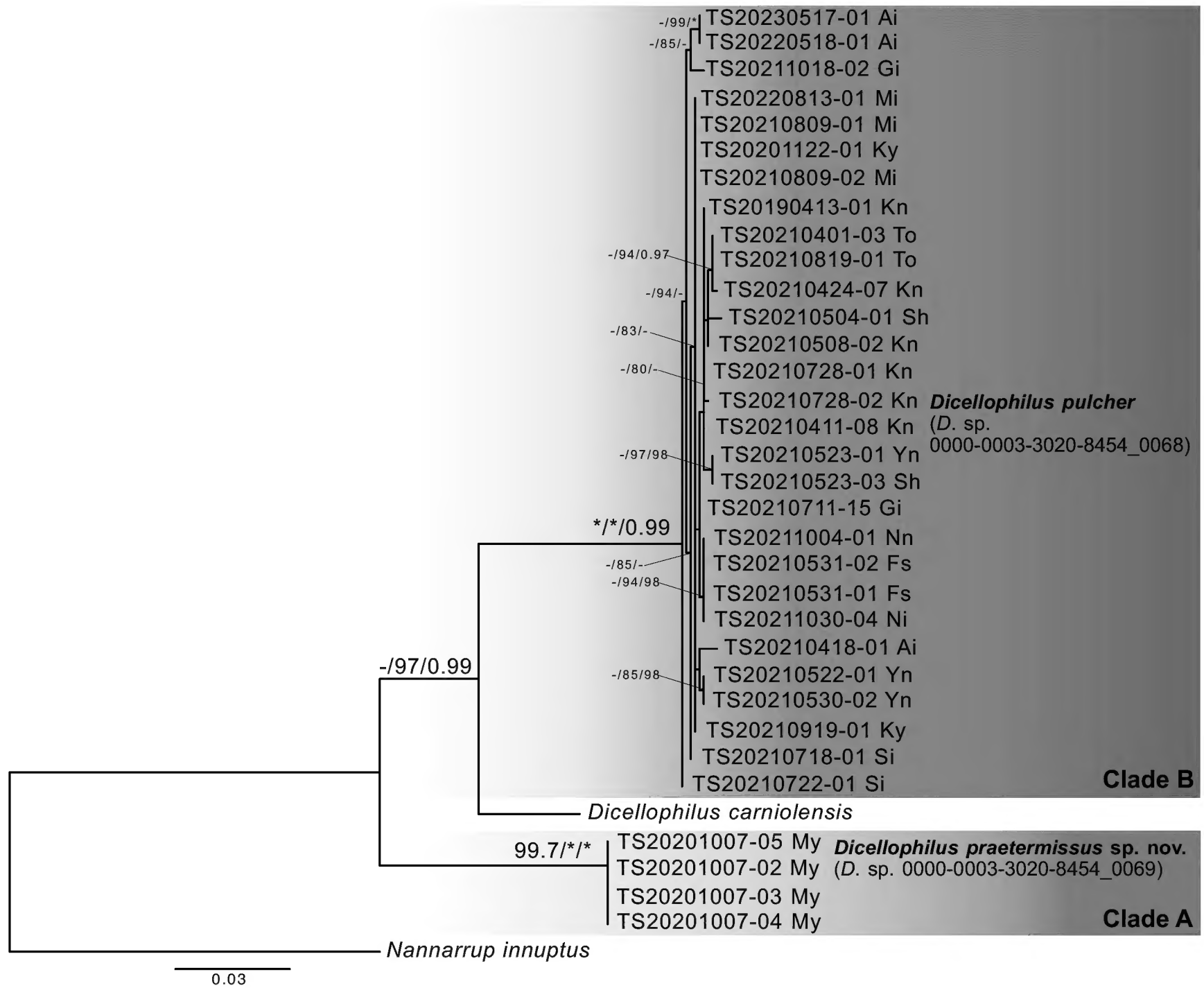

Figure 5. Maximum-likelihood tree of *Dicellophilus* based on the dataset of *28S*. Nodal values are obtained from the ultrafast bootstrap (UFBoot), SH-like approximate likelihood ratio test (SH-aLRT), and posterior probability (PP). The asterisk (*) indicates 100% in UFBoot, SH-aLRT, and 1.0 in PP. Hyphen (-) indicates lower than 95% in UFBoot, 80% in SH-aLRT, or 0.95 in PP. Nodal values are not shown when UFBoot, SH-aLRT, and PP values are <95%, <80%, and <0.95, respectively. The unit of evolutionary distance is the number of base substitutions per site. A broken square shows that the clade consisted of specimens from eastern Honshu. Abbreviations: Ai = Aichi Pref.; Fs = Fukushima Pref.; Gi = Gifu Pref.; Kn = Kanagawa Pref.; Ky = Kyoto Pref.; Mi = Mie Pref.; My = Miyagi Pref.; Ni = Niigata Pref.; Nn = Nagano Pref.; Sh = Shizuoka Pref.; Si = Saitama Pref.; To = Tokyo Pref.; Yn = Yamanashi Pref.

In addition, the 23 adult specimens, including a specimen from the type locality of *D. pulcher* (Subashiri, Oyama, Suntou-gun, Shizuoka Pref.), had the following diagnostic characteristics of *D. pulcher* (Uliana et al. 2007; Bonato et al. 2010a): trunk segments without dark patches; head 1.2–1.4 times as long as it is wide; cephalic plate with a markedly convex lateral margin; clypeus with densely scattered setae; palaclypeal suture evidently converging posteriorly; transverse suture uniformly rounded at center; mandible with 5–7 lamellae; forcipular tarsungulum with evident and variably spaced notches; and 41 pairs of legs.

On the other hand, four specimens of Clade A (TS20201007-02, TS20201007-03, TS20201007-04, and TS20201007-05) were morphologically different from the specimens of Clade B based on the following characteristics: both ends of transverse suture not evidently convex forward; long rather than wide trochanteroprefemur; wide rather than long metasternite (Table 3).

Taxonomic account

Family Mecistocephalidae Bollman, 1893

Genus *Dicellophilus* Cook, 1896

Dicellophilus praetermissus sp. nov.

https://zoobank.org/8A967E03-A5B0-4495-A0E9-6CE1298F3E3D

Figs 6–13

New Japanese name: Date-hirozujimukade

DI. *Dicellophilus* sp. 0000-0003-3020-8454_0069

Type material. ***Holotype.*** 1 adult male, Baba, Akiu-machi, Taihaku-ku, Sendai-shi, Miyagi Pref., Japan (38°16.33'N, 140°32.69'E), 7 October 2020, coll. Sho Tsukamoto (labeled as TS20201007-02), deposited at the Collection of Myriapoda, Department of Zoology, **NSMT**.

Paratype. 1 adult male, Baba, Akiu-machi, Taihaku-ku, Sendai-shi, Miyagi Pref., Japan (38°16.33'N, 140°32.69'E), 7 October 2020, coll. Sho Tsukamoto

Table 3. Morphological comparison between *D. pulcher* and *D. praetermissus* sp. nov.

Putative species identification code	Species identified in the present study	Both ends of transverse suture	The width to length ratio of trochanteroprefemur	The width to length ratio of sternite of ULBS
Dicellophilus sp. 0000-0003-3020-8454_0068	*Dicellophilus pulcher* (Kishida, 1928)	evidently convex forward	1: 0.9–1.1	1: 1.0–1.3
Dicellophilus sp. 0000-0003-3020-8454_0069	*Dicellophilus praetermissus* sp. nov.	not evidently convex	1: 1.3–1.4	1: 0.66–1.0

Figure 6. Habitus of *Dicellophilus praetermissus* sp. nov., paratype (TS20201007-05). Photo by Joe Kutsukake.

(labeled as TS20201007-03), 1 adult female, Baba, Akiu-machi, Taihaku-ku, Sendai-shi, Miyagi Pref., Japan (38°16.33'N, 140°32.69'E), 7 October 2020, coll. Sho Tsukamoto (labeled as TS20201007-04), 1 adult male, Baba, Akiu-machi, Taihaku-ku, Sendai-shi, Miyagi Pref., Japan (38°16.33'N, 140°32.69'E), 7 October 2020, coll. Sho Tsukamoto (labeled as TS20201007-05), deposited at **MNHAH**.

Etymology. The species name is a masculine adjective derived from "overlooked" in Latin. Since the description by Kishida (1928) of *D. pulcher* (as *Mecistocephalus pulcher*), this new species has been overlooked for 90 years, despite documentation of its distribution as *Dicellophilus* in the Sendai-shi, Miyagi Pref. (Takakuwa 1940).

Diagnosis. Trunk segments without dark patches; head 1.4 times as long as wide; lateral margin of cephalic plate abruptly converged posteriorly; clypeus with densely scattered setae; palaclypeal suture evidently converging posteriorly; both ends of transverse suture uniformly rounded; mandible with 6 lamellae; forcipular trochanteroprefemur longer than wide, with one small distal denticle; forcipular tarsungulum with evident and variably spaced notches; metatergite subtrapezoidal; metasternite trapezoidal, wide rather than long; forty-one pairs of legs.

Description. ***General features*** (Fig. 6): Body about 50 mm long (holotype ca 52 mm), gradually attenuated posteriorly, almost uniformly pale yellow, with head and forcipular segment ocher.

Cephalic capsule (Fig. 7A, B): Cephalic plate ca 1.3–1.4× as long as wide; lateral margins markedly convex; posterior margin straight; areolate part visible only at anterior margin; scutes approximately isometric and up to 20 μm wide in 50 mm long specimen; both ends of transverse suture uniformly rounded or slightly convex forward; setae up to ca 300 μm long. Clypeus ca 2.3–2.5× as wide as long, with lateral margins complete, anterior part areolate, with scutes ca 30 μm wide in 50 mm long specimen, clypeal areas absent; clypeus with about 200 setae on most part except lateral and posterior margins; clypeal plagulae undivided by mid-longitudinal areolate stripe. Anterior and distolateral parts of pleurites areolate, without setae, non-areolate part extending forwards distinctly beyond labrum. Side-pieces of labrum not in contact, anterior margin not concave posteriorly but horizontally, divided into anterior and posterior alae by chitinous line, with longitudinal stripes on posterior alae, with medial tooth, and short fringe on posterior margin of side-pieces; mid-piece ca 6.2 times as long as wide, lateral margin concaved.

Antenna (Fig. 8A–H): Antenna with 14 articles, when stretched, ca 2.7–3.2× as long as head length. Intermediate articles longer than wide. Distal part of article areolate, remaining surface not areolate in article I–XIII. Article XIV ca 2.1–2.5× as long as wide, ca 1.1–1.5× as long as article XIII. Setae on articles VIII–XVI denser than articles I–VII. Setae gradually shorter from article VIII to XIV, up to ca 290 μm long on article I, up to ca 270 μm long on article VIII and < 75 μm long on article XIV. Article XIV with two types of sensilla; apical sensilla (arrows in Fig. 8G, H) ca 25 μm long, with wide flat ring at mid-length; club-like (arrowheads in Fig. 8G, H) sensilla ca 15 μm long, clustered in distal part of internal and external sides of article. Rows of spine-like basal sensilla (the 'sensilla microtrichoidea' of Ernst 1983, 1997, 2000) absent on antennal article VI and X. A few pointed sensilla, up to 7.5 μm long, on both dorso-external and ventro-internal position, close to distal margin of articles II, V, IX and XIII.

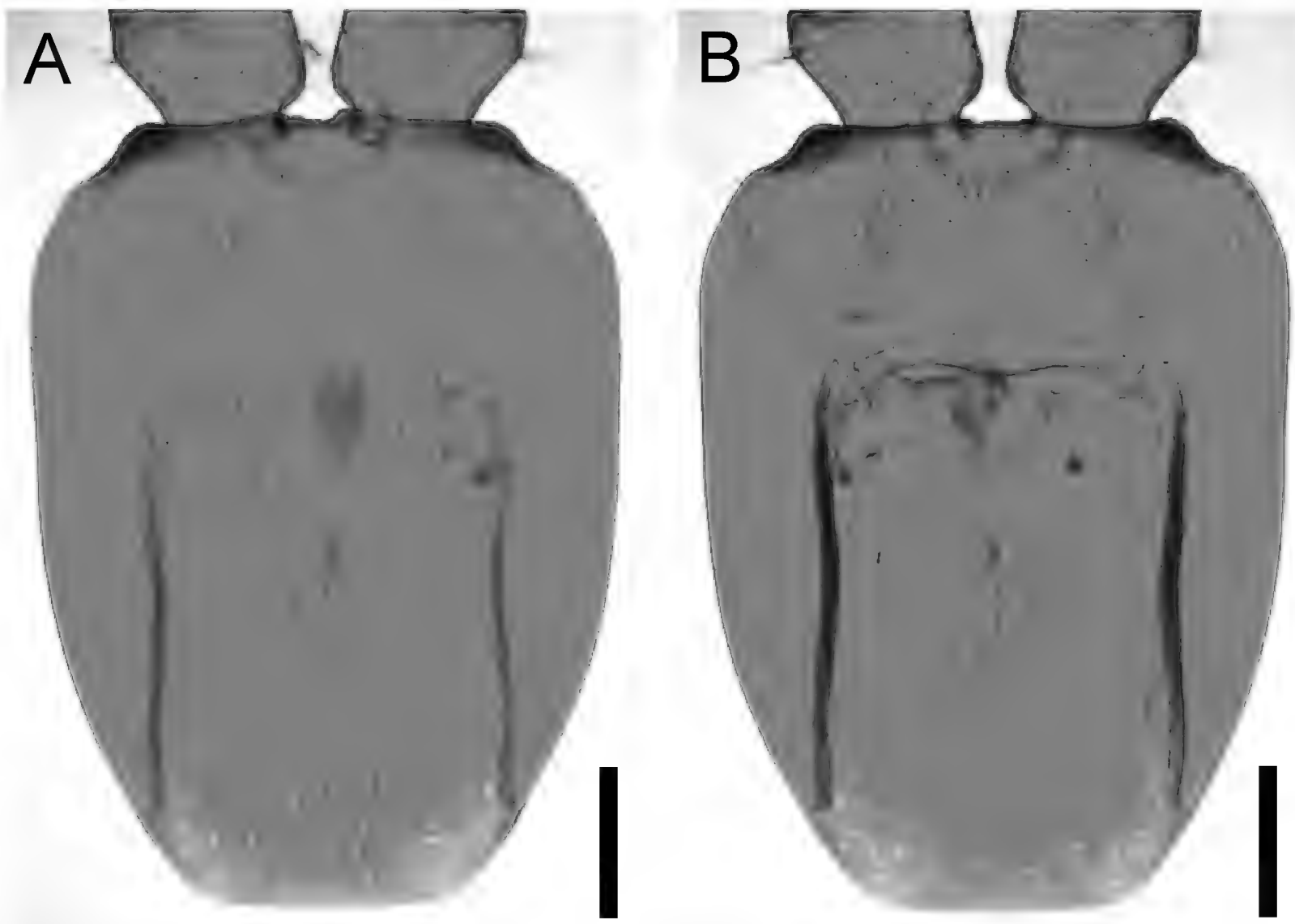

Figure 7. *Dicellophilus praetermissus* sp. nov., holotype (TS20201007-02) **A** cephalic plate, dorsal **B** clypeus, and clypeal pleurite, ventral. Scale bars: 0.5 mm.

Mandible (Fig. 9A): Five–six pectinate lamellae present; first lamellae with at least 4 elongated teeth. Anterior surface hairy.

First maxillae (Fig. 9B): Coxosternite medially divided but slightly, without setae, without projection on antero-external corners, non-areolate. Coxal projections well developed, with ca 20 setae along internal margin, distal lobe subtriangular. Telopodite uni-articulated and hyaline distally, with 5–6 setae. No lobes on either coxosternite or telopodites.

Second maxillae (Fig. 9B): Coxosternite medially undivided, without suture but areolated on isthmus, with 4+4 setae along anterior margin, with about 25 setae on isthmus, with about 15 setae on lateral margin and posterior corners, anterior margin concave, with metameric pores on posterior part. Telopodites tri-articulate, reaching medial projections and telopodites of first maxillae. Claw of telopodite present.

Forcipular segment (Fig. 10A–E): Tergite trapezoidal, ca 1.3–1.4× as wide as long, with lateral margins converging anteriorly, areolation mainly along two marginal lateral and anterior bands and two paramedian posterior areas, gradually fading into central non-areolate surface; ca 0.5–0.6× as wide as cephalic plate and ca 0.4–0.5× as wide as tergite 1; 3+2 setae of similar length arranged in an anterior row, and ca 20 setae of similar length arranged symmetrically in a posterior row. Mid-longitudinal sulcus of tergite not visible. Pleurite 1.8–1.9× as long as the tergite; dorsal ridge sclerotized; anterior tip (scapular point) well behind anterior margin of coxosternite, and only slightly projecting. Cerrus composed of a group of 10–20 setae on each side of anterodorsal surface of coxosternite, but no paramedian rows of setae. Exposed part of coxosternite ca 1.2× as wide as long; anterior margin with shallow medial concavity and with one pair of denticles; coxopleural sutures complete in entire ventrum, sinuous and diverging anteriorly; chitin-lines absent; condylar processes of forcipular coxosternite well developed. Trochanteroprefemur ca 1.3–1.4× as long as wide; with a pigmented tubercle at distal internal margin. Intermediate articles distinct, with a tubercle on femur and tibia. Tarsungulum with well-pigmented basal tubercle on dorsal surface; both external and internal margins uniformly curved, except for moderate mesal basal bulge; ungulum not distinctly flattened; internal margin of ungulum evidently crenulated, with variably spaced notches. Elongated poison calyx lodged inside intermediate forcipular articles.

Leg-bearing segments (Fig. 11A–D): Forty-one pairs of legs present. Metatergite 1 slightly wider than subsequent one, with two paramedian sulci visible on tergites of anterior half of body, with pretergite. No paratergites. Legs of first pair much smaller than following ones; claws simple, uniformly bent, with 2 accessory spines; posterior spine shorter than anterior spine; with a subsidiary spine near posterior spine (arrow in Fig. 11D). Metasternites slightly longer than wide. Sternal sulcus evident on segment II, but fading towards posterior segments, anteriorly not furcate. No ventral glandular pores on each metasternite.

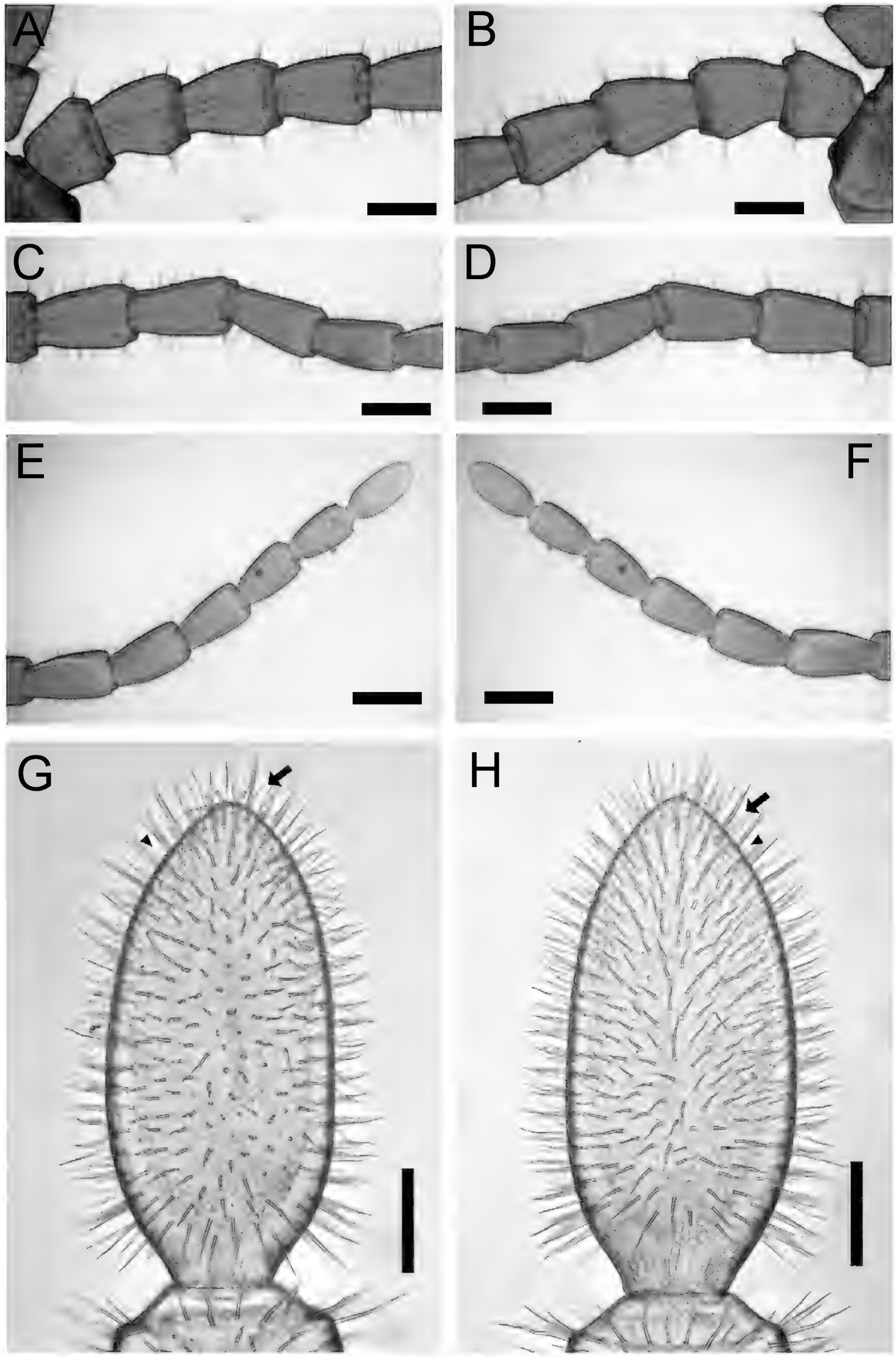

Figure 8. *Dicellophilus praetermissus* sp. nov. **A–F.** Holotype (TS20201007-02) **G, H.** Paratype (TS20201007-04) **A.** Antennal articles I–IV, dorsal; **B.** Antennal articles I–IV, ventral; **C.** Antennal articles V–VIII, dorsal; **D.** Antennal articles V–III, ventral; **E.** Antennal articles IX–XIV, dorsal; **F.** Antennal articles IX–XIV, ventral; **G.** Antennal article XIV, dorsal; **H.** Antennal article XIV, ventral. Arrows indicate apical sensillum; arrowheads indicate club-like sensillum. Scale bars: 0.5 mm (**A–F**); 0.1 mm (**G, H**).

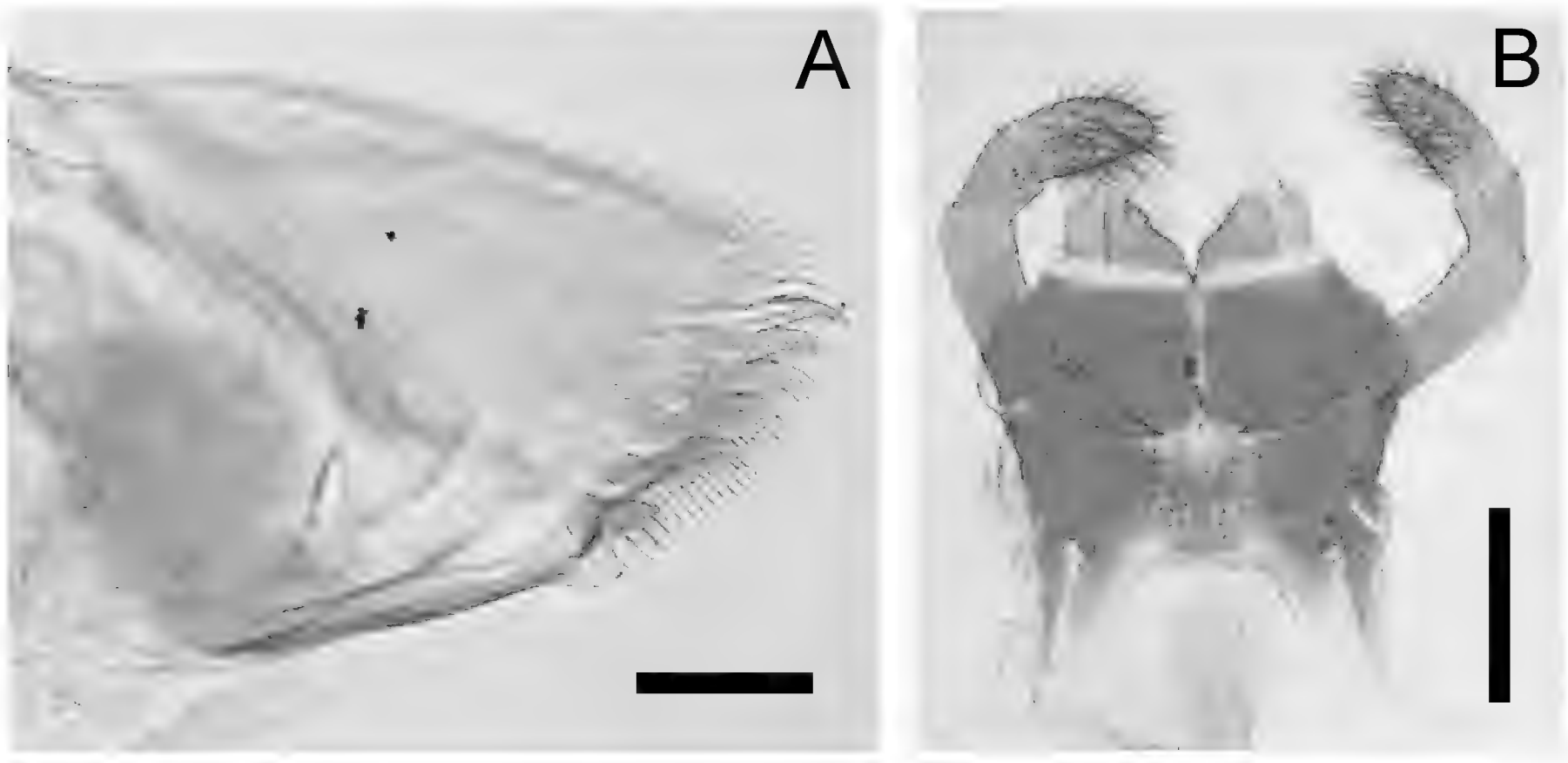

Figure 9. *Dicellophilus praetermissus* sp. nov., holotype (TS20201007-02) **A.** Left mandible, ventral; **B.** Maxillae complex, ventral. Scale bars: 0.1 mm (**A**); 0.5 mm (**B**).

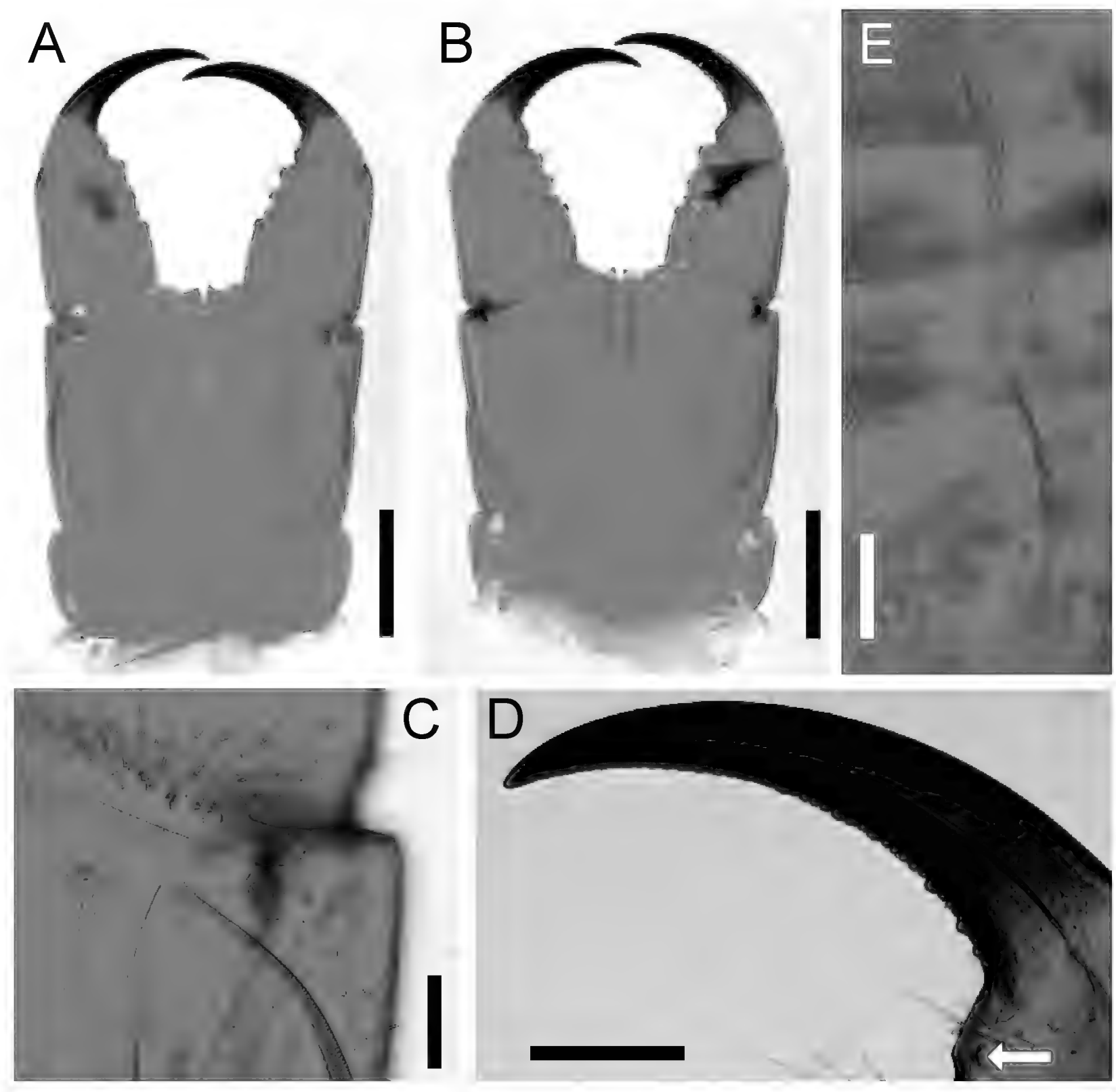

Figure 10. *Dicellophilus praetermissus* sp. nov., holotype (TS20201007-02). **A.** Forcipular segment, dorsal; **B.** Forcipular segment, ventral; **C.** Right condylar process of forcipular coxosternite, dorsal; **D.** Right forcipular tarsungulum, dorsal; **E.** Poison calyx, dorsal. The arrow indicates the basal tubercle of the forcipular tarsungulum. Scale bars: 0.5 mm (**A, B**); 0.2 mm (**C**); 0.3 mm (**D**); 0.1 mm (**E**).

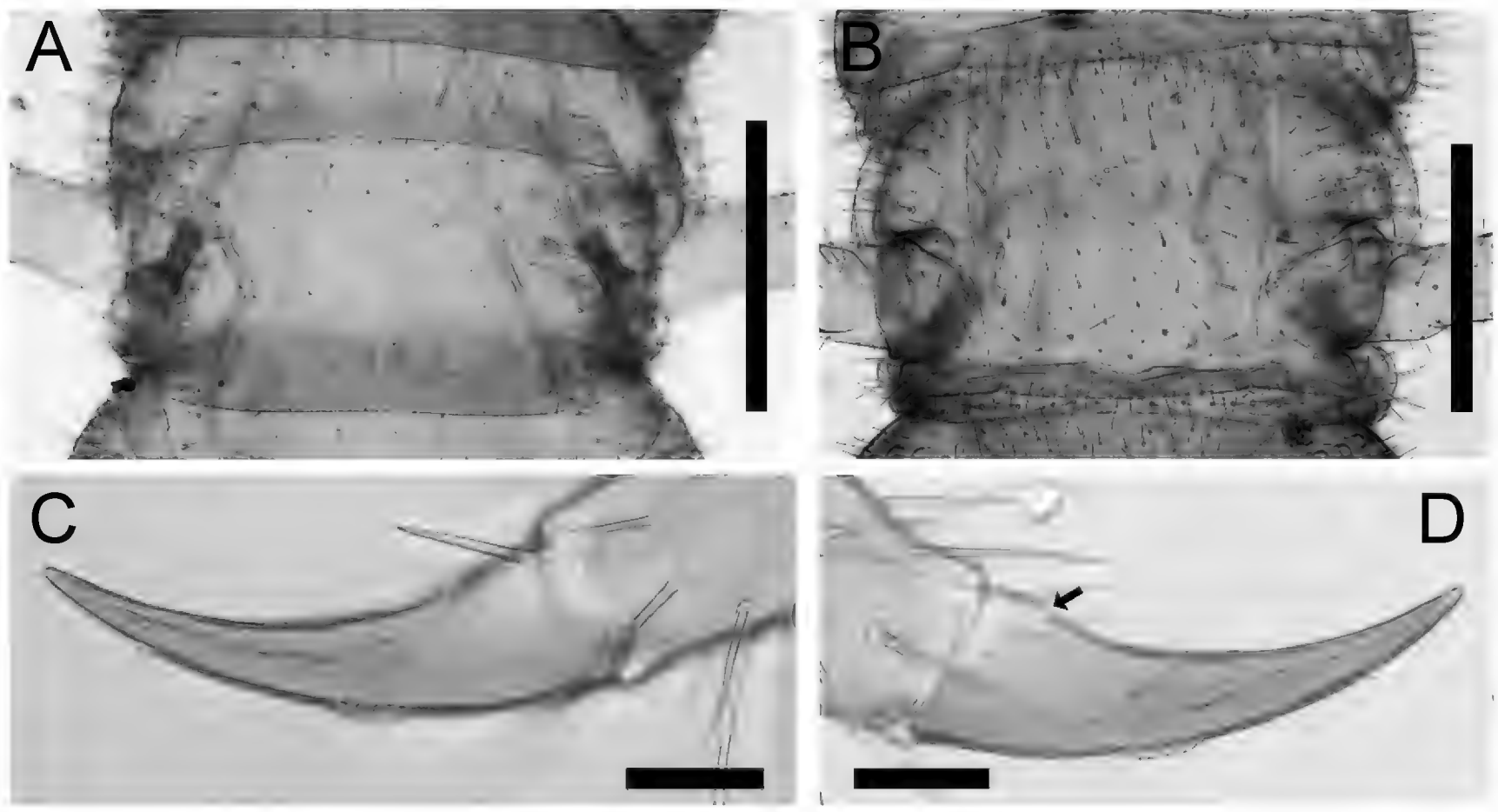

Figure 11. *Dicellophilus praetermissus* sp. nov., holotype (TS20201007-02). **A.** Tergite of leg-bearing segment 40, dorsal; **B.** Sternite of leg-bearing segment 40, ventral; **C.** Pretarsus of left leg 40, anterolateral. **D.** Pretarsus of left leg 2, posterolateral. The arrow indicates a subsidiary spine. Scale bars: 0.5 mm (**A, B**); 0.1 mm (**C, D**).

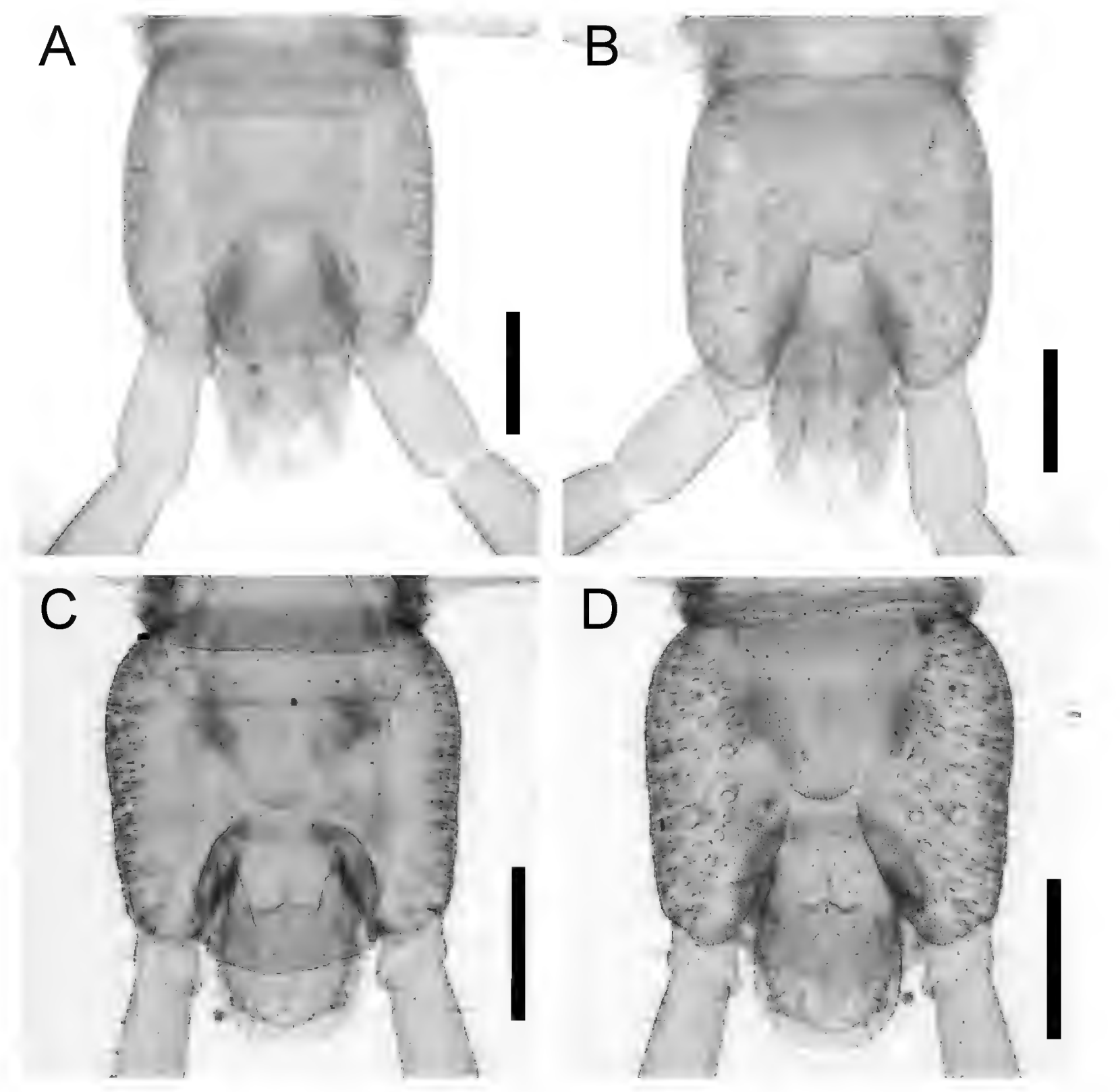

Figure 12. *Dicellophilus praetermissus* sp. nov. **A, B.** Holotype (TS20201007-02) **C, D.** Paratype (TS20201007-04) **A, C.** Ultimate leg-bearing segment and postpedal segment, dorsal; **B, D.** Ultimate leg-bearing segment and postpedal segment, ventral. Scale bars: 0.5 mm.

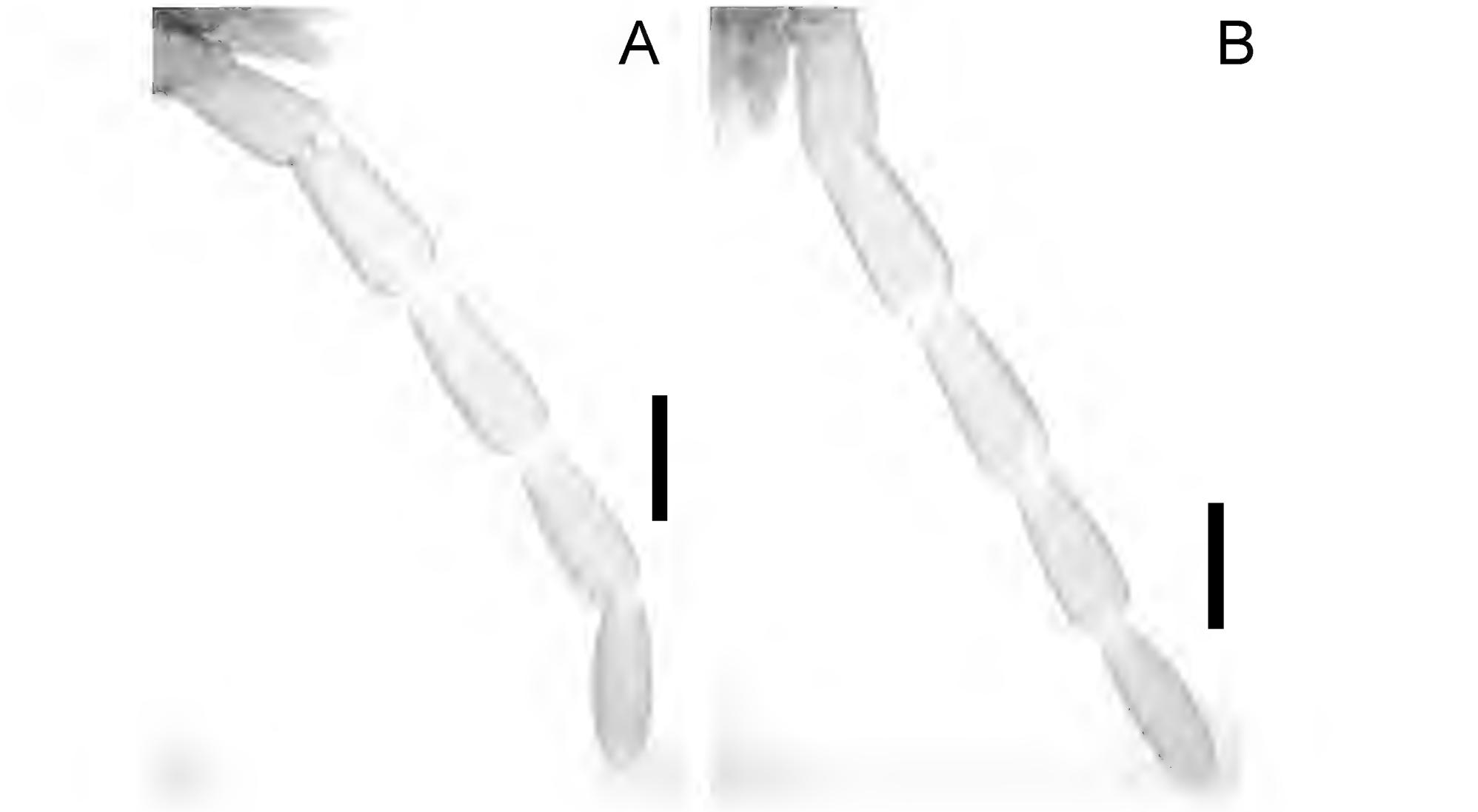

Figure 13. *Dicellophilus praetermissus* sp. nov., holotype (TS20201007-02). **A.** Left ultimate leg, dorsal; **B.** Left ultimate leg, ventral. Scale bars: 0.5 mm.

Ultimate leg-bearing segment (Figs 12A–D, 13A, B): Pretergite accompanied by pleurites. Metatergite subtrapezoidal, ca 1.2–1.5× as long as wide; lateral margins converging posteriorly. Coxopleuron ca 1.8–2.3× as long as metasternite; coxal organs of each coxopleuron opening through ca 70 independent pores, placed ventrally; distinctly larger pore (macropore) near center of the ventral side. Metasternite trapezoidal, ca 1.1–1.5× as wide as long, anteriorly ca 3.0–3.6× as wide as posteriorly; lateral margins converging backward straightly; setae almost arranged symmetrically, dense on posterior margin. In male holotype (TS20201004-02), telopodite ca 11.5× as long as wide, ca 1.6× as long, and ca 1.3× as wide as penultimate telopodite, with six articles; tarsus 2 ca 3.3× as long as wide and ca 1.1× as long as tarsus 1; setae arranged uniformly, < 200 μm long; pretarsus without claw. In female paratype (TS20201004-04), telopodite ca 13.5× as long as wide, ca 1.8× as long, and ca 1.3× as wide as penultimate telopodite, with six articles; tarsus 2 ca 5.2× as long as wide and ca 1.3× as long as tarsus 1; setae arranged uniformly, < 300 μm long; pretarsus without claw.

Male postpedal segments (Fig. 12A, B): Two gonopods, very widely separated from one another, conical in outline, bi-articulated with sutures, covered with setae. Anal pore present.

Female postpedal segments (Fig. 12C, D): Two gonopods basally touching, subtriangular, bi-articulated with sutures, covered with setae. Anal pore present.

Distribution. Only known from the type locality.

Remarks. *Dicellophilus praetermissus* sp. nov. most closely resembles *D. pulcher* but is distinguishable by the following combination of characteristics: both ends of transverse suture not evidently convex forward; the longer than wide trochanteroprefemur; the wide rather than long metasternite (Table 3).

The record of *D. latifrons* Takakuwa, 1934 (= *D. pulcher*) from Sendai, Miyagi Pref. (Takakuwa 1940) requires confirmation of its identification.

Dicellophilus pulcher (Kishida, 1928)

Figs 14–16

Mecistocephalus pulcher Kishida, 1928: Kishida 1928, 300.
Dicellophilus latifrons: Takakuwa 1934a, 707; Takakuwa 1934b, 355; Takakuwa 1934c, 878.
Dicellophilus japonicus: Verhoeff 1934, 32.
Tygarrup monoporus: Shinohara 1961, 212.
Dicellophilus pulcher: Uliana et al. 2007, 27; Bonato et al. 2010, 525.

DI. *Dicellophilus* sp. 0000-0003-3020-8454_0068

Material examined. See Table 1.

Diagnosis. Mainly based on Bonato et al. (2010a), Uliana et al. (2007), and the present study. Trunk segments without dark patches; head 1.2–1.4 times as long as wide (Fig. 14A, B); lateral margin of cephalic plate abruptly converged posteriorly; clypeus with densely scattered setae (Fig. 14B); paraclypeal suture evidently converging posteriorly (Fig. 14B); both ends of transverse suture convexed forward (Fig. 14A); mandible with 5–7 lamellae; forcipular trochanteroprefemur almost as long as wide, with one small distal denticle (Fig. 15A, B); forcipular tarsungulum with evident and variably spaced notches; metatergite subtrapezoidal (Fig. 16A); metasternite trapezoidal, longer than wide (Fig. 16B); forty-one pairs of legs.

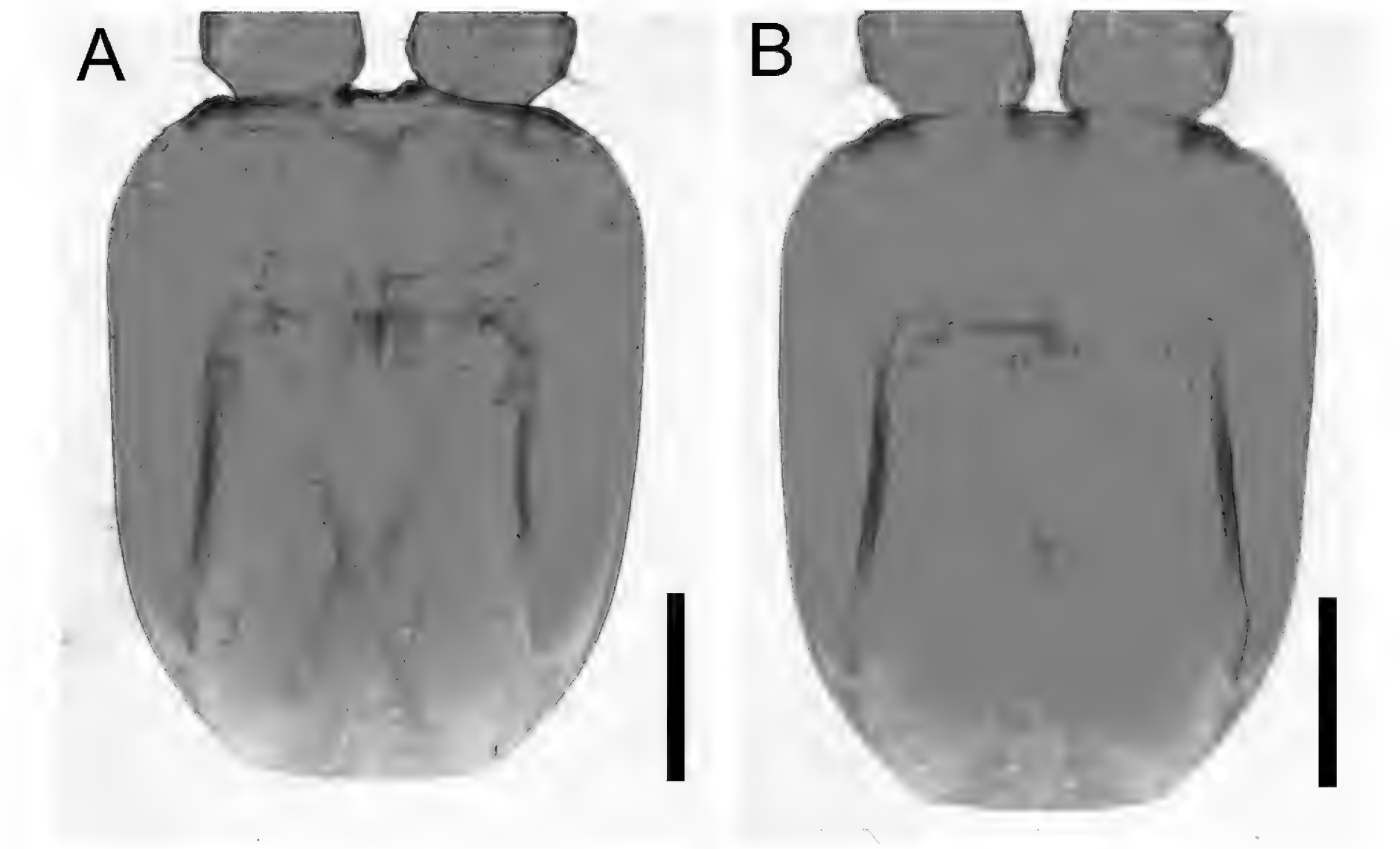

Figure 14. *Dicellophilus pulcher* (TS20210504-01). **A.** Cephalic plate, dorsal; **B.** Clypeus, and clypeal pleurite, ventral. Scale bars: 0.5 mm.

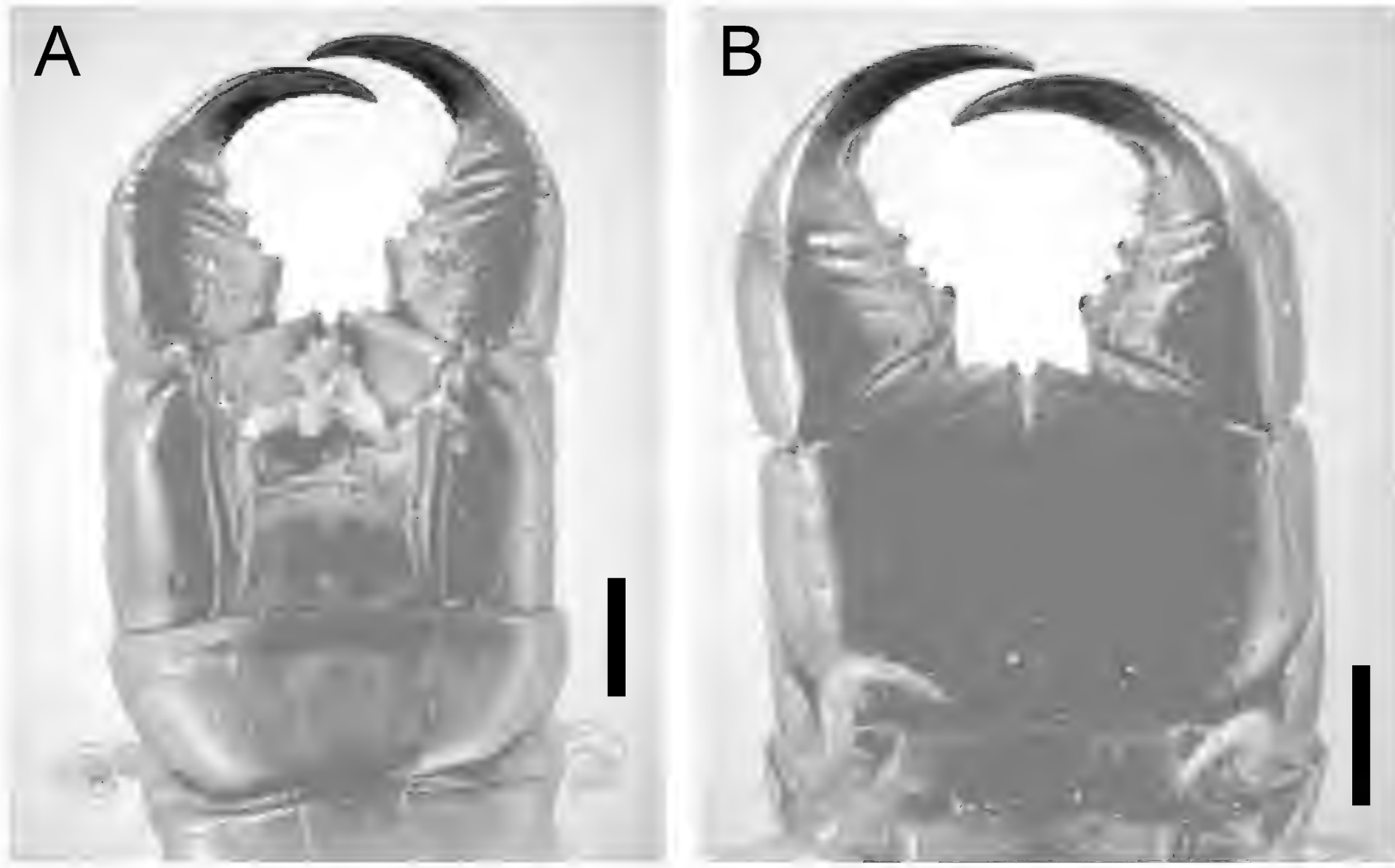

Figure 15. *Dicellophilus pulcher* (TS20210504-01). **A.** Forcipular segment, dorsal; **B.** Forcipular segment, ventral. Scale bars: 0.5 mm.

Type locality. The first section of the Subashiri trail of Mt. Fuji, Shizuoka Pref., Japan (Kishida 1928).

Distribution. Honshu (Fukushima Pref. to Hyogo Pref.).

Remarks. See remarks and the diagnosis of *D. praetermissus* sp. nov. for confirming how to distinguish *D. pulcher* from *D. praetermissus* sp. nov.

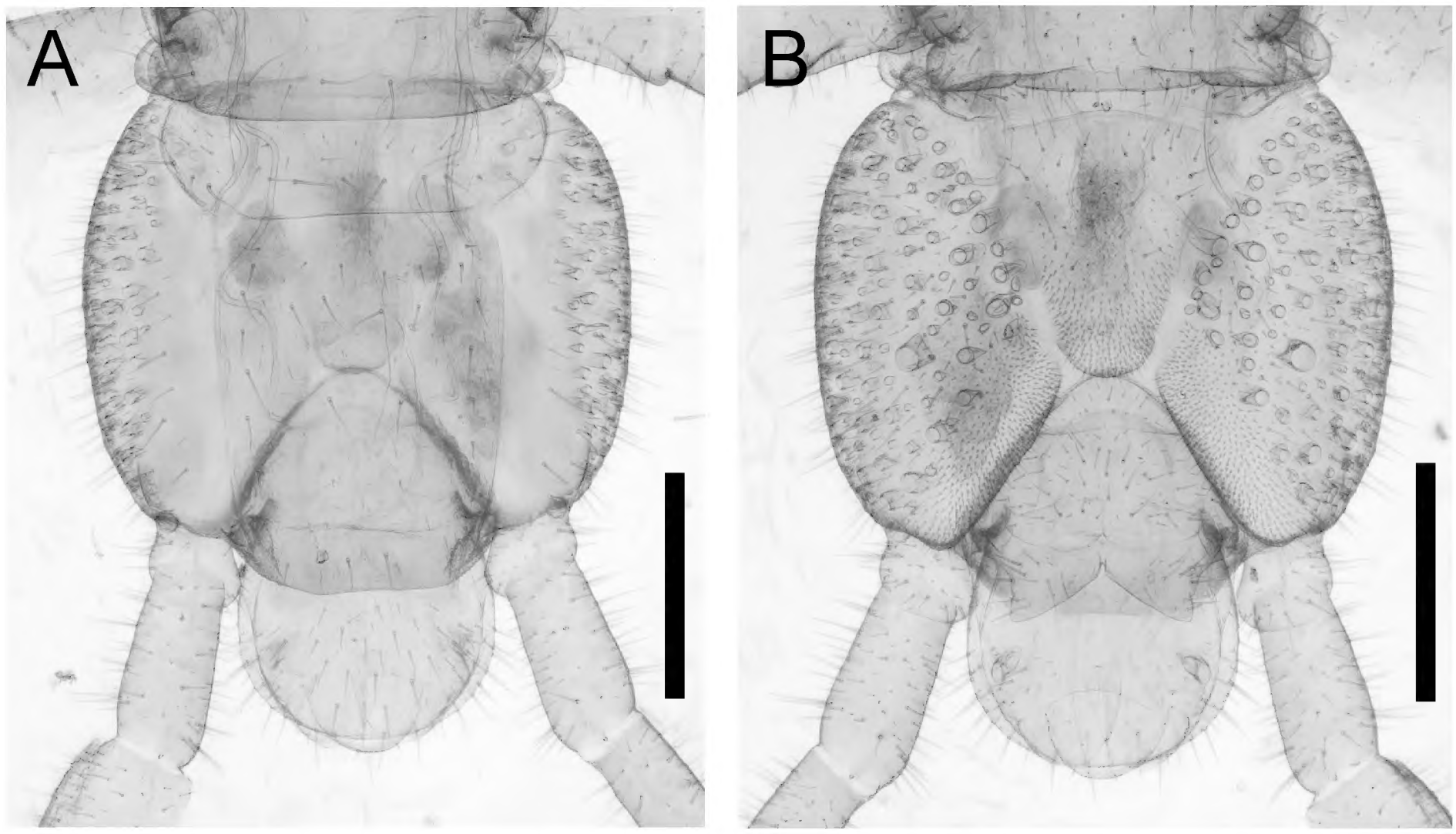

Figure 16. *Dicellophilus pulcher* (TS20210504-01). **A.** Ultimate leg-bearing segment and postpedal segment, dorsal; **B.** Ultimate leg-bearing segment and postpedal segment, ventral. Scale bars: 0.5 mm.

There are three junior synonyms under *D. pulcher*, which were synonymized by previous authors based on morphological examination (Takakuwa 1940; Shinohara 1983; Uliana et al. 2007): *D. latifrons* Takakuwa, 1934; *D. japonicus* Verhoeff, 1934; *Tygarrup monoporus* Shinohara, 1961. *Dicellophilus latifrons* Takakuwa, 1934, which was described in a key to Japanese and Taiwanese species of Mecistcephalidae by Takakuwa (1934a), was later described by Takakuwa (1934b, c) as a new species. Takakuwa (1934a) did not designate a type locality for *D. latifrons*, and Takakuwa (1934b, c) listed the localities: "Kaibara (Hyogo)" (= Tamba City, Hyogo Pref.), "Masudo (bei Tokyo)" (possibly misread of Masuko-mura, currently in Akiruno-shi, Tokyo Pref.), "Komono (Miye)" (= Komono-cho, Mie Pref.), "Ikao (Gumma)" (= Ikahocho, Shibukawa-shi, Gunma Pref.), "Ōta (Gumma)" (= Ota-shi, Gunma Pref.), "Odawara (Kanagawa)" and "Suwa (Nagano)" (annotated by Jonishi and Nakano 2022). Considering the geographic distribution of *D. latifrons* and *D. pulcher* sensu stricto, *D. latifrons* is a junior synonym of *D. pulcher*. *Dicellophilus japonicus* Verhoeff, 1934, was described based on a specimen from "Tokyo" (Verhoeff 1934) and later regarded as a junior synonym of *D. latifrons* based on the comparison of diagnostic characteristics (Takakuwa 1940; Shinohara 1983). Considering the geographic distribution of *D. japonicus* and *D. pulcher* and the phylogenetic analyses of the present study, including TS20181214-01, TS20191006-02, TS20210401-03, and TS20210819-01 from Tokyo Pref., it is not conflicting that *D. japonicus* is a junior synonym of *D. pulcher*. *Tygarrup monoporus* Shinohara, 1961, which is identical to the juvenile of *D. pulcher*, according to Uliana et al. (2007), was described based on the specimen from Manazuru-machi, Ashigarashimo-gun, Kanagawa Pref. (Shinohara 1961). Considering the geographic distribution of *T. monoporus* and *D. pulcher* and the phylogenetic analyses of the present study, including TS20210728-02, which was collected at a linear distance of approximately 13 km from the type locality and could be identified as *T. monoporus*, *T. monoporus* can also be regarded as a junior synonym of *D. pulcher*.

Discussion

Species hypothesis for Japanese *Dicellophilus*

No POTU delimitation hypotheses proposed by ASAP corresponded well to the principle in steps I–IV. This is because each of those hypotheses involves many POTUs, which were separated from each other with a K2P distance lower than the intermorphospecific threshold. Although Clade B could be divided into many more POTUs, such partitioning hypotheses can be rejected as oversplitting in accordance with the species delimitation criteria in step IV with the intermorphospecific threshold (21% in *COI*). Therefore, two putative species were recognized in the 38 *D. pulcher* specimens examined in steps I–IV, and they can be separately labeled as follows: *Dicellophilus* sp. 0000-0003-3020-8454_0068 (= Clade B; hereafter referred to as *D.* sp. 0068) and *D.* sp. 0000-0003-3020-8454_0069 (= Clade A; hereafter referred to as *D.* sp. 0069, Table 3, Figs 2–5).

Only one validly named species of *Dicellophilus* from Japan, *D. pulcher*, was described on the basis of a specimen from the Subashiri trail of Mt. Fuji, Shizuoka Pref. (Kishida 1928). *Dicellophilus* sp. 0068 involves a specimen

from the type locality (TS20210504-01) and shares the number of pairs of legs, the presence of macropores on the coxopleuron, and a wide forcipular trochanteroprefemur with the original description (including figures) of *D. pulcher*. Therefore, *D.* sp. 0068 is conferrable to *D. pulcher*. By contrast, *D.* sp. 0069 can be regarded as a new species based on morphological comparison with other congeners, including *D. pulcher*. This new species is described in the "Taxonomic account" section under the name *Dicellophilus praetermissus* sp. nov. (step V); see also the taxonomic discussion of junior synonyms of *D. pulcher*.

Oversplit of the number of POTUs by ASAP

As mentioned in the result section, many POTUs were divided from the *COI* dataset of *Dicellophilus* examined in the present study. When taking into account the overall genetic diversity of all examined specimens of *Dicellophilus*, i.e., *D. pulcher*, *D. carniolensis* and *D. praetermissus* sp. nov. (maximum genetic divergence in K2P: 24%), the genetic diversity within the morphospecies *D. pulcher* alone is quite high (15%).

Possibly, such an oversplit of POTU would have been caused by the algorithm ASAP and the quite high genetic divergence of *D. pulcher* in the dataset. According to Puillandre et al. (2021), ASAP is a hierarchical clustering algorithm. Each subgroup was separated depending on the average pairwise distance between subgroups and within the subgroup, sample size, and a coalescent mutation rate. Based on this algorithm, the distribution of genetic distances will affect the result of the number of species (= POTUs). In detail, when there is high genetic diversity within one morphospecies compared to the whole dataset, the morphospecies will be divided into several POTUs, in accordance with the possibility of panmixia (*p*-value).

POTUs are divided by the possibility of panmixia, so it can be expected that each POTU will be a biological species. However, each POTU within the morphospecies *D. pulcher* detected in the present study is not regarded as a species until morphological evidence is discovered.

Distribution of *Dicellophilus* in Japan

Dicellophilus specimens examined in Japan were collected from 34°33'N to 38°16'N on Honshu within a latitudinal band, which is congeners' distribution. The authors and their collaborators have collected *Dicellophilus* exclusively from Miyagi Pref. to Kyoto Pref. but not from other areas, despite a comprehensive field trip in Japan (Fig. 1). Therefore, the distribution of *Dicellophilus* in Japan should be restricted from Miyagi Pref. to Kyoto Pref. (see Remarks of *D. pulcher* in this paper; Takakuwa 1940; Uliana et al. 2007).

According to the molecular phylogenetic analyses of *Dicellophilus* specimens in Japan, it is possible that there are two large populations among *D. pulcher*, viz., specimens from Eastern Honshu (Fukushima Pref. to Shizuika Pref. and one specimen from Gifu Pref.) and those from western Honshu (Gifu Pref. to Kyoto Pref.), because the monophyly was supported by the phylogenetic analysis based on the concatenated and *COI* datasets, respectively. However, the boundary between two populations is still not clear due to the lack of field surveys in the central part of Honshu.

In field surveys conducted by the authors in Japan, *D. praetermissus* sp. nov. was collected only in Sendai-shi, Miyagi Pref. (the northern part of Honshu). It is also noteworthy that *D. pulcher* has yet to be collected from the northern part of Honshu (from Aomori Pref. to Miyagi Pref). This result of field surveys shows that the distribution of *D. praetermissus* sp. nov. may segregate from *D. pulcher*, but further field surveys are needed around Miyagi Pref.

Acknowledgments

We are grateful to Dr Masaru Nonaka (visiting researcher of Tokyo Metropolitan University), Dr Namiki Kikuchi (Toyohashi Museum of Natural History), Dr Takahiro Yoshida (assistant professor of Tokyo Metropolitan University), Mr Joe Kutsukake (Tokyo Metropolitan University), Mr Koshi Kawamoto (Tokyo Metropolitan University), Ms Mayu Susukida, Mr Ryo Miyata, Mr Tatsumi Suguro (Keio Yochisha Elementary School), Mr Tomoki Sumino, and Mr Fukube Sumino for collecting and providing *Dicellophilus* specimens. We are further grateful to Dr Namiki Kikuchi and Mr Joe Kutsukake for assisting in collecting and taking photographs of *Dicellophilus praetermissus* sp. nov., respectively. We thank two reviewers for providing valuable comments and suggestions. We also would like to thank Enago (www.enago.jp) for the English language review. This study was supported by the following funds: the Fund for the Promotion of Joint International Research (Fostering Joint International Research (B), JSPS KAKENHI, no. 22KK0087, leader: Katsuyuki Eguchi, FY2022–2025), Grant-in-Aid for Scientific Research (C) (JSPS KAKENHI, no 23K05299, Leader: Emiko Oguri, FY2023–2026), the Tokyo Metropolitan University Fund for TMU Strategic Research (leader: Noriaki Murakami, FY2020–FY2022), and the Asahi Glass Foundation (leader: Katsuyuki Eguchi, FY2017–FY2023).

References

Aberer AJ, Kobert K, Stamatakis A (2014) ExaBayes: Massively parallel Bayesian tree inference for the whole-genome era. Molecular Biology and Evolution 31(10): 2553–2556. https://doi.org/10.1093/molbev/msu236

Bonato L (2011) Order Geophilomorpha. In: Minelli A (Ed.) Treatise on Zoology— Anatomy, Taxonomy, Biology. The Myriapoda I, Brill, Leiden, 407–443.

Bonato L, Foddai D, Minelli A (2003) Evolutionary trends and patterns in centipede segment number based on a cladistic analysis of Mecistocephalidae (Chilopoda: Geophilomorpha). Systematic

Entomology 28(4): 539–579. https://doi.org/10.1046/j.1365-3113.2003.00217.x

Bonato L, Dányi L, Minelli A (2010a) Morphology and phylogeny of *Dicellophilus*, a centipede genus with a highly disjunct distribution (Chilopoda: Mecistocephalidae). Zoological Journal of the Linnean Society 158(3): 501–532. https://doi.org/10.1111/j.1096-3642.2009.00557.x

Bonato L, Edgecombe GD, Lewis JGE, Minelli A, Pereira LA, Shelley RM, Zapparoli M (2010b) A common terminology for the external anatomy of centipedes (Chilopoda). ZooKeys 69: 17–51. https://doi.org/10.3897/zookeys.69.737

Bonato L, Drago L, Murienne J (2014) Phylogeny of Geophilomorpha (Chilopoda) inferred from new morphological and molecular evidence. Cladistics 30(5): 485–507. https://doi.org/10.1111/cla.12060

Bonato L, Bortlin F, De Zen G, Decker P, Linder EN, Orlando M, Spelda J, Voigtländer K, Wesener T (2023) Towards elucidating species diversity of European inland *Strigamia* (Chilopoda: Geophilomorpha): a first reassessment integrating multiple lines of evidence. Zoological Journal of the Linnean Society 199(4): 945–966. https://doi.org/10.1093/zoolinnean/zlad070

Boyer SL, Giribet G (2007) A new model Gondwanan taxon: Systematics and biogeography of the harvestman family Pettalidae (Arachnida, Opiliones, Cyphophthalmi), with a taxonomic revision of genera from Australia and New Zealand. Cladistics 23(4): 337–361. https://doi.org/10.1111/j.1096-0031.2007.00149.x

Dayrat B (2005) Towards integrative taxonomy. Biological Journal of the Linnean Society. Linnean Society of London 85(3): 407–415. https://doi.org/10.1111/j.1095-8312.2005.00503.x

Dyachkov YuV, Bonato L (2022) Morphology and distribution of the Middle Asian centipede genus *Krateraspis* Lignau, 1929 (Chilopoda, Geophilomorpha, Mecistocephalidae). ZooKeys 1095: 143–164. https://doi.org/10.3897/zookeys.1095.80806

Edgecombe GD, Giribet G (2006) A century later – a total evidence re-evaluation of the phylogeny of scutigeromorph centipedes (Myriapoda, Chilopoda). Invertebrate Systematics 20(5): 503–525. https://doi.org/10.1071/IS05044

Ernst A (1983) Die Ultrastruktur der Sinneshaare auf den Antennen von *Geophilus longicornis* Leach (Myriapoda, Chilopoda). IV. Die Sensilla microtrichoidea. Zoologische Jahrbücher. Abteilung für Anatomie 109: 521–546.

Ernst A (1997) Sensilla microtrichoidea – mutmaßliche 'Stel-lungsrezeptoren' an der Basis der Antennenglieder des Chilopoden Geophilus longicornis Leach. Verhandlungen der Deutschen Zoologischen Gesellschaft 90: 274.

Ernst A (2000) Structure and function of different cuticular sensilla in the centipede *Geophilus longicornis* Leach. Fragmenta Faunistica, Warszawa 43(Suppl.): 113–129.

Guindon S, Dufayard JF, Lefort V, Anisimova M, Hordijk W, Gascuel O (2010) New algorithms and methods to estimate maximum-likelihood phylogenies: Assessing the performance of PhyML 3.0. Systematic Biology 59(3): 307–321. https://doi.org/10.1093/sysbio/syq010

Hoang DT, Chernomor L, von Haeseler A, Minh BQ, Vinh LS (2018) UFBoot2: Improving the ultrafast bootstrap approximation. Molecular Biology and Evolution 35(2): 518–522. https://doi.org/10.1093/molbev/msx281

Jonishi T, Nakano T (2022) Correct Authorships, Synonymies, and Remarks on the Type Series of Fourteen Names of Centipedes Introduced by Yoshioki Takakuwa in 1934 and *Mecistocephalus takakuwai* (Chilopoda: Geophilomorpha and Scolopendromorpha). Species Diversity : An International Journal for Taxonomy, Systematics, Speciation, Biogeography, and Life History Research of Animals 27(1): 71–81. https://doi.org/10.12782/specdiv.27.71

Joshi J, Karanth KP (2012) Coalescent Method in Conjunction with Niche Modeling Reveals Cryptic Diversity among Centipedes in the Western Ghats of South India. PLoS ONE 7(8): e42225. https://doi.org/10.1371/journal.pone.0042225

Katoh K, Standley DM (2013) MAFFT multiple sequence alignment software version 7: Improvements in performance and usability. Molecular Biology and Evolution 30(4): 772–780. https://doi.org/10.1093/molbev/mst010

Kishida K (1928) Ch. 6. Chilopoda. In: Sengen Shrine (Ed.) Animals of Mt. Fuji. Kokinshoin, Tokyo, 290–303. [in Japanese]

Kumar S, Stecher G, Li M, Knyaz C, Tamura K (2018) MEGA X: Molecular evolutionary genetics analysis across computing platforms. Molecular Biology and Evolution 35(6): 1547–1549. https://doi.org/10.1093/molbev/msy096

Murienne J, Edgecombe GD, Giribet G (2010) Including secondary structure, fossils and molecular dating in the centipede tree of life. Molecular Phylogenetics and Evolution 57(1): 301–313. https://doi.org/10.1016/j.ympev.2010.06.022

Nguyen LT, Schmidt HA, von Haeseler A, Minh BQ (2015) IQ-TREE: A Fast and Effective Stochastic Algorithm for Estimating Maximum-Likelihood Phylogenies. Molecular Biology and Evolution 32(1): 268–274. https://doi.org/10.1093/molbev/msu300

Padial JM, Miralles A, De la Riva I, Vences M (2010) The integrative future of taxonomy. Frontiers in Zoology 7(1): 16. https://doi.org/10.1186/1742-9994-7-16

Peretti E, Cecchin C, Fusco G, Gregnanin L, Kos I, Bonato L (2022) Shedding light on species boundaries in small endogeic animals through an integrative approach: species delimitation in the centipede *Clinopodes carinthiacus* (Chilopoda: Geophilidae) in the south-eastern Alps. Zoological Journal of the Linnean Society 196(2): 902–923. https://doi.org/10.1093/zoolinnean/zlac008

Puillandre N, Brouillet S, Achaz G (2021) ASAP: Assemble species by automatic partitioning. Molecular Ecology Resources 21(2): 609–620. https://doi.org/10.1111/1755-0998.13281

Rambaut A, Drummond AJ, Xie D, Baele G, Suchard MA (2018) Posterior summarization in Bayesian phylogenetics using Tracer 1.7. Systematic Biology 67(5): 901–904. https://doi.org/10.1093/sysbio/syy032

Satria R, Kurushima H, Herwina H, Yamane S, Eguchi K (2015) The trap-jaw ant genus *Odontomachus* Latreille (Hymenoptera: Formicidae) from Sumatra, with a new species description. Zootaxa 4048(1): 1–36. https://doi.org/10.11646/zootaxa.4048.1.1

Shinohara K (1961) Taxonomical and morphological studies of Myriapoda VII. Two new species of Mecistocephalidae (Chilopoda). Zoological Magazine 70(7): 212–216. [in Japanese with English Resume]

Shinohara K (1983) Revision on the scientific names of Japanese myriapods. V. On the *Dicellophilus pulcher* (Kishida). Takakuwaia 15: 5–6.

Siriwut W, Edgecombe GD, Sutcharit C, Panha S (2015) The Centipede Genus Scolopendra in Mainland Southeast Asia: Molecular Phylogenetics, Geometric Morphometrics and External Morphology as Tools for Species Delimitation. PLoS ONE 10(8): e0135355. https://doi.org/10.1371/journal.pone.0135355

Siriwut W, Edgecombe GD, Sutcharit C, Tongkerd P, Panha S (2016) A taxonomic review of the centipede genus *Scolopendra* Linnaeus, 1758 (Scolopendromorpha, Scolopendridae) in mainland Southeast

Asia, with description of a new species from Laos. ZooKeys 590: 1–124. https://doi.org/10.3897/zookeys.590.7950

Takakuwa Y (1934a) The family Mecistocephalidae of Japan, I. Botany and Zoology 2(4): 706–712. [in Japanese]

Takakuwa Y (1934b) Neue japanische Mecistocephalidae. Annotationes Zoologicae Japonenses 14: 355–363.

Takakuwa Y (1934c) The family Mecistocephalidae of Japan, II. Botany and Zoology 2(5): 878–884. [in Japanese]

Takakuwa Y (1940) Fauna Nipponica 9 (8, 1). Geophilomorpha. Sanseido, Tokyo, 156 pp. [in Japanese]

The International Commission on Zoological Nomenclature (1999) International Code of Zoological Nomenclature. The International Trust for Zoological Nomenclature 1999, The Natural History Museum - Cromwell Road - London SW7 5BD – UK. https://code.iczn.org/authorship/article-51-citation-of-names-of-authors/?frame=1

Tsukamoto S (2023) Phylogenetic and Taxonomic Study of Japanese and Taiwanese Species of the Centipede Family Mecistocephalidae (Chilopoda: Geophilomorpha). PhD Thesis, Graduate School of Science, Tokyo Metropolitan University, Tokyo.

Tsukamoto S, Shimano S, Murakami T, Hiruta SF, Yamasaki T, Eguchi K (2019) A new species of the genus *Arrup* from a limestone cave in Akiyoshi-dai, Western Japan (Chilopoda, Geophilomorpha, Mecistocephalidae). ZooKeys 830: 33–51. https://doi.org/10.3897/zookeys.830.33060

Tsukamoto S, Nguyen AD, Eguchi K (2021a) Confirmation of the phylogenetic position of the unique geophilomorph genus *Vinaphilus* Tran, Tran & Bonato, 2019 (Chilopoda: Geophilomorpha: Gonibregmatidae) by molecular phylogenetic analyses, with two new species from the Central Highlands of Vietnam. Zoologischer Anzeiger 293: 74–88. https://doi.org/10.1016/j.jcz.2021.05.004

Tsukamoto S, Hiruta SF, Eguchi K, Liao J-R, Shimano S (2021b) A new amphibious species of the genus *Scolopendra* Linnaeus, 1758 (Scolopendromorpha, Scolopendridae) from the Ryukyu Archipelago and Taiwan. Zootaxa 4952(3): 465–494. https://doi.org/10.11646/zootaxa.4952.3.3

Tsukamoto S, Shimano S, Eguchi K (2022) Two new species of the dwarf centipede genus *Nannarrup* Foddai, Bonato, Pereira & Minelli, 2003 (Chilopoda, Geophilomorpha, Mecistocephalidae) from Japan. ZooKeys 1115: 117–150. https://doi.org/10.3897/zookeys.1115.83946

Uliana M, Bonato L, Minelli A (2007) The Mecistocephalidae of the Japanese and Taiwanese islands (Chilopoda: Geophilomorpha). Zootaxa 1396(1): 1–84. https://doi.org/10.11646/zootaxa.1396.1.1

Verhoeff KW (1934) Beiträge zur Systematik und Geographie der Chilopoden. Zoologische Jahrbücher. Abteilung für Systematik 66: 1–112.

Xiong B, Kocher TD (1991) Comparison of mitochondrial DNA sequences of seven morphospecies of black flies (Diptera: Simuliidae). Genome 34(2): 306–311. https://doi.org/10.1139/g91-050